OVERLAND FLOW ANALYSIS FOR A SIMULATED VEGETATED SURFACE

Annual Allotment Agreement No. 14-01-0001

Charles E. Rice
Assistant Professor of Agricultural Engineering
Oklahoma State University

Period Covered by Research Investigation
July 1, 1968 through June 30, 1969

OVERLAND FLOW ANALYSIS FOR A SIMULATED
VEGETATED SURFACE

Annual Allotment Agreement No. 14-01-0001-

Charles E. Rice
Assistant Professor of Agricultural Engineering
Oklahoma State University

Period Covered by Research Investigation
July 1, 1968 through June 30, 1969

ABSTRACT

OVERLAND FLOW ANALYSIS FOR A SIMULATED
VEGETATED SURFACE

Uniform and spatially varied flows were investigated
using a 44-foot long, 1.325-foot wide, rectangular flume
located indoors. Tests were conducted at channel slopes
of one, two, three, and four per cent. In order to approx-
imate a close-growing mat type grass such as bermudagrass,
the channel bottom was lined with artificial grass, of
trade name PERMA-GRASS. The lateral inflow, designed to
approximate natural rainfall, was applied by spray nozzles
along the longitudinal axis of the flume. Rainfall rates
of approximately 1.3, 2.3, 4.2, and 8.0 inches per hour
were studied.

Three flow regimes were observed and were noted as
constant-velocity, mixed, and turbulent. For the experi-
mental surface studied the depth can be predicted in the
constant-velocity and mixed flow regimes of overland flow
from the relationships of Y versus Q obtained from the
uniform flow tests. In the turbulent flow regime the
momentum equation and the energy (Bernoulli) equation
accurately predicted the water surface profiles. A sim-
plified momentum equation was used and it predicted the
depth change as accurately as the complete momentum equa-
tion. When the bottom slope is assumed equal to the
energy slope and equivalent discharge uniform flow Manning
n values are used in the Manning equation, good predictions
of the water surface profile for turbulent steady state
increasing spatially varied flow result for these tests.

The raindrop impact caused an increase in the roughness
for the spatially varied flows compared to the uniform flows.
The presence of rainfall, more than the intensity, seemed
to affect the roughness, so that no relationship between
rainfall intensity and Manning n could be derived.

KEYWORDS: Spatially varied flow*/vegetated surface/uniform
           flows/energy equation/momentum equation/Manning
           equation/raindrop impact.

This research project was terminated before its scheduled completion date. The reason for this was that after some tests had been completed, it was evident that all of the project objectives could not be achieved with the physical apparatus and measurement equipment being used in the conduct of the tests. Some of the physical phenomena that were necessary for complete achievement of the project objectives were of such a small magnitude that they could not be measured with the equipment at our disposal. However, some of the project objectives were achieved and the results obtained should be of interest and should be helpful in further study and analysis of overland flow phenomena.

The proposed project objectives as set forth in the Research Project Proposal are:

A. To determine the functional relationship between watershed roughness (expressed as some appropriate friction factor such as Manning's n) and the depth of flow, rainfall intensity (raindrop impact), and slope of surface profile for a simulated vegetated surface for spatially varied steady flow and spatially varied unsteady flow (overland flow).

B. An analysis of overland flow using the continuity and momentum equations as the expressions to completely define the time distribution of runoff (hydrograph) from a simulated vegetated sur-

face.

C. Solution of the complete continuity and momentum
    equations by numerical methods subject to the
    following:

    1. Use of friction factors obtained from
        uniform flow condition to evaluate the
        friction slope in the momentum equation.
        This assumes a constant friction factor
        for the range of conditions studied.

    2. Use of friction factors obtained from
        spatially varied steady flow conditions
        to evaluate the friction slope in the
        momentum equation. This assumes that
        the friction factor varies with depth,
        rainfall intensity, and slope of sur-
        face.

D. Comparison of the hydrographs obtained by methods
    mentioned above to the hydrographs of runoff ob-
    tained from the experimental facility. This will
    permit evaluation of results obtained using
    friction factors determined by the above mentioned
    methods.

E. Adjustment of the friction factor in the friction
    slope of the equations until the predicted hydro-
    graphs duplicate the experimentally determined
    hydrographs. This should permit determination of
    the actual friction factor relationship for the
    different variable combinations of overland flow
    from a simulated vegetated surface.

The objectives sought, background information, the research problem and procedure used, the methods of analysis, and the results and conclusions are presented in the accompanying masters thesis which is submitted as the main text for the Research Project Technical Termination Report.

No publications have resulted from the research project at this time, but a paper is currently being prepared for submission for publication.

STEADY STATE INCREASING SPATIALLY

VARIED FLOW OVER A SIMULATED

VEGETATED SURFACE

By

PAUL KEITH RODMAN

Bachelor of Science

Oklahoma State University

Stillwater, Oklahoma

1968

Submitted to the faculty of the
Graduate College
of the Oklahoma State University
in partial fulfillment of the
requirements for the degree
of
MASTER OF SCIENCE
August, 1969

Name: Paul Keith Rodman   Date of Degree: August 1, 1969

Institution: Oklahoma State University Location: Stillwater, Oklahoma

Title of Study: STEADY STATE INCREASING SPATIALLY VARIED FLOW OVER A
                 SIMULATED VEGETATED SURFACE

Pages: 90   Candidate for Degree of Master of Science

Major Field: Agricultural Engineering

Scope of Study: Uniform and spatially varied flows were investigated
     using a 44-foot long, 1.325-foot wide, rectangular flume located
     indoors. Tests were conducted at channel slopes of one, two, three,
     and four per cent. In order to approximate a close-growing mat
     type grass such as bermudagrass, the channel bottom was lined with
     artificial grass, of trade name PERMA-GRASS. The lateral inflow,
     designed to approximate natural rainfall, was applied by spray
     nozzles along the longitudinal axis of the flume. Rainfall rates
     of approximately 1.3, 2.4, 4.2, and 8.0 inches per hour were studied.
     Uniform flow tests were conducted with flows from about .1 to 42
     gallons per minute, while total flow in the rainfall tests varied
     from about .7 to 27 gallons per minute.

Findings and Conclusions: Three flow regimes were observed and were
     noted as constant-velocity, mixed, and turbulent. For the experi-
     mental surface studied the depth can be predicted in the constant-
     velocity and mixed flow regimes of overland flow from the relation-
     ships of Y versus Q obtained from the uniform flow tests. In the
     turbulent flow regime the momentum equation and the energy
     (Bernoulli) equation accurately predicted the water surface pro-
     files. A simplified momentum equation was used and it predicted
     the depth change as accurately as the complete momentum equation.
     When the bottom slope is assumed equal to the energy slope and
     equivalent discharge uniform flow Manning n values are used in
     the Manning equation, good predictions of the water surface profile
     for turbulent steady state increasing spatially varied flow result
     for these tests. The accuracy of predicting the water surface
     profiles in the turbulent flow regime is dependent on how well the
     surface roughness is represented by the Manning n values used.

     The raindrop impact caused an increase in the roughness for the
     spatially varied flows compared to the uniform flows. The pres-
     ence of rainfall, more than the intensity, seemed to affect the
     roughness, so that no relationship between rainfall intensity and
     Manning n could be derived.

ADVISER'S APPROVAL_____

STEADY STATE INCREASING SPATIALLY

VARIED FLOW OVER A SIMULATED

VEGETATED SURFACE

Thesis Approved:

_____
Thesis Adviser

_____

_____
Dean of the Graduate College

ACKNOWLEDGEMENTS

The author would like to express appreciation to his adviser, Professor Charles E. Rice, for his competent guidance throughout the study. His suggestions and assistance were especially helpful with the collection and analysis of data and in the preparation of the thesis.

Special thanks is extended to Dr. James E. Garton for his comments and suggestions throughout the study.

The author is grateful to Mr. Will Hamilton for construction work and for calibration of the water measuring devices.

The assistance of Mr. Ward Shaklee and Mr. David Shaklee with the collection and analysis of data is appreciated. Mr. Jess Hoisington, Mr. Clyde Skoch, and Mr. Norvil Cole gave valuable technical advice and aid. Mr. Jack Fryrear is acknowledged for his excellent preparation of illustrative

material.

Sincere thanks is extended to Mrs. Linda Parrish for her conscientious typing of the thesis.

TABLE OF CONTENTS

LIST OF TABLES

LIST OF FIGURES

CHAPTER I

INTRODUCTION

Overland flow is the initial phase of surface runoff
from rainfall. Interest in the subject has continued be-
cause hydrologists seek improved methods for runoff pre-
diction. The primary hydrologic problem in the design of
hydraulic structures, whether it be the design of the
principal spillway for a small farm pond, a highway culvert,
a vegetated waterway, or drainage structures for an airport
runway, is the determination of the time distribution of
surface runoff and peak flow from the drainage area con-
cerned for a given rainfall intensity and duration. A
better understanding of overland flow would improve runoff
prediction and should aid in the interpretation of soil
erosion phenomena and therefore in the evaluation of land
treatments used for the control of erosion.

The use of a strictly hydraulic procedure for pre-
dicting overland flow is beset with many difficulties.
Overland flow is both unsteady and spatially varied since
it is supplied by rain and depleted by infiltration, neither
of which is necessarily constant with respect to time or
location. Most of the previous methods of predicting the
time distribution of runoff have been by empirical,

1

statistical, or routing methods because of the complexity of the problem or the quantities of data involved. Today high speed digital computers have made practical the use of numerical methods which can be applied to the momentum or energy equation for spatially varied flow.

Much of the current research is being applied to watershed models with experimental facilities which usually have concrete or masonite type materials to represent the watershed surface. Also, many of the researchers assume, or at least use, a constant friction factor such as Chezy's C or Manning's n to evaluate the friction slope in the momentum equation. The reason for this probably is that at this time information is not available relating the friction factor for overland flow to the variables involved.

Many researchers emphasize the need for a functional relationship between the watershed roughness and other variables, especially the depth of flow, rainfall intensity or raindrop impact, and surface slope. Complete, accurate solutions to the energy or momentum equations may not be realized until these friction relationships are known for different watershed surfaces, that is, turf, sod, asphalt, concrete, and so forth. The major emphasis of this thesis and research is the determination of the friction relationship for a simulated vegetated surface. Hopefully these results can be applied to overland flow from natural watersheds.

Limitations of the Study

Though this thesis is limited to steady state increasing spatially varied flow, continuous readings were taken during the unsteady state.

The experimental data were obtained using a 44-foot variable slope rectangular flume located indoors. The flume was 1.325 feet wide, with polished masonite sidewalls. In order to approximate a close-growing mat type grass such as bermudagrass, the channel bottom was lined with artificial grass, of trade name PERMA-GRASS. The channel slope was varied from one to four percent. The lateral inflow, designed to approximate natural rainfall, was applied by spray nozzles located along the longitudinal axis of the flume. The spray was ejected upward and fell into the channel. Rainfall rates of approximately 1.3, 2.6, 4.2, and 8.0 inches per hour were studied. Base flow was introduced at the upstream end of the channel for uniform flow tests and for the spatially varied flow tests where an initial flow was desired. Uniform flow tests were conducted up to a maximum discharge of about 42 gallons per minute; maximum base flow for rainfall tests was about 27 gallons per minute.

Objectives

1. To determine the functional relationship between watershed roughness, which is expressed by

Manning's n, and the depth of flow, rainfall intensity or raindrop impact, and the physical slope for a simulated vegetated surface for steady state increasing spatially varied flow.

2. To determine whether n values obtained from uniform flow tests can be used in the Manning equation to predict water surface profiles for similar discharge, steady state increasing spatially varied flows.

3. To determine the applicability of the energy and momentum equations for predicting water surface profiles for steady state increasing spatially varied flow.

4. To compare the surface profiles determined by the above methods to those observed in the experimental facility.

5. To adjust the friction factors in the energy and momentum equations until the predicted water surface profiles agree with those determined experimentally.

Definition of Symbols

Symbol	Quantity	Dimensions
a	area of flow per foot of width	ft
A	area of flow	ft^2
$\overline{A}$	average area of flow	ft^2
b	channel width	ft

Symbol	Quantity	Dimensions
E	specific energy	ft
F_f	shear force	lb
g	acceleration due to gravity	ft/sec^2
G	arbitrary function	nonhomogeneous
H_{fx}	friction head	ft
H_v	velocity head	ft
i	hydraulic gradient	dimensionless
K_{cv}	coefficient, constant-velocity flow equation	nonhomogeneous
K_1	coefficient, laminar flow equation	nonhomogeneous
K_m	coefficient, mixed flow equation	nonhomogeneous
K_p	coefficient of permeability	ft/sec
K_{pa}	coefficient, K_p times a constant area	nonhomegeneous
K_t	coefficient, turbulent flow equation	nonhomogeneous
M	exponent, mixed flow equation	nonhomogeneous
n	Manning's n, roughness coefficient	nonhomogeneous
n_p	predicted Manning n value	nonhomogeneous
q	discharge per unit width	ft^2/sec
Q	discharge	ft^3/sec
r	distance downstream from the origin	ft
R	hydraulic radius	ft
RENO	Reynolds number	dimensionless
S_f	energy slope	dimensionless
S_{fx}	energy slope at any point x	dimensionless

Symbol	Quantity	Dimensions
$\overline{S}_{fx}$	effective energy slope from x = 0 to x	dimensionless
S_o	bottom slope	dimensionless
t	time	sec
V	velocity of flow	ft/sec
w	unit weight of water	lb/ft^3
W	weight of water	lb
x	distance from some reference point	ft
y	depth of flow	ft
Y_{ef}	effective depth	ft
Z	bottom elevation	ft
$\propto$	Coriolis velocity coefficient	dimensionless
λ	coefficient of friction	dimensionless
ϕ	flow added per unit x increment	ft^3/sec

CHAPTER II

REVIEW OF LITERATURE

This chapter is concerned with basic hydraulic theory and previous research pertinent to the study. Spatially varied flow, Manning's Equation, increasing spatially varied flow water surface prediction equations, and general regimes of flow are the primary subjects discussed.

Spatially Varied Flow

In spatially varied flow, water runs in or out along the course of flow. Flow is varied if the depth changes along the length of the channel. Varied flow may be classified as steady or unsteady, and further differentiated as rapidly or gradually varied. The flow is gradually varied unless the depth changes abruptly over a relatively short distance.

The water which enters or departs during spatially varied flow causes disturbances in the energy or momentum content of the flow. Therefore, the hydraulic behavior of such flow is more complicated than that of a constant discharge. Also, the hydraulic behavior of increasing spatially varied flow and decreasing spatially varied flow is somewhat different (4).

Increasing spatially varied flow occurs in rainfall

runoff. After the initial requirements of interception and

depression storage have been met, a buildup of minute

depths of water occurs and is referred to as detention

storage. This stored water collects in small rivulets which

convey the water to small channels (6). This runoff water

can be considered as overland flow. According to Ree (22),

"Overland flow is runoff moving as a sheet over a plane

surface to the nearest collector channel." Among the im-

portant factors influencing the time response of a water-

shed, and thus overland flow, to imposed rainfall are rain-

fall intensity, storm duration, watershed slope and length,

and hydraulic roughness (6).

Manning Equation, Manning's n

Uniform Flow Applications

During the nineteenth century, R. Manning presented an

equation for uniform flow in open channels. The present

well-known form of the equation is:

$$V = \frac{1.49}{n} \, R^{2/3} \, S_f^{1/2} \tag{1}$$

where V is the mean velocity in feet per second, R is the

hydraulic radius in feet, S_f is the slope of the energy

line, and n is the coefficient of roughness, known as

Manning's n. Due to its simple form and the satisfactory

results produced for practical applications, the Manning

Equation has become the most popular of all uniform flow

equations for open channel flow (4).

The greatest difficulty in applying the Manning Equation is in the determination of the roughness coefficient n. Without experimentation this can only be an estimate. Among the factors affecting n are surface roughness and vegetation. Surface roughness is a function of the size and shape of the grains of the material forming the wetted perimeter and producing a retarding effect on the flow. Vegetation may be considered as a type of surface roughness, but it also reduces the capacity of the channel and retards the flow. The effect of the vegetation depends on its height, density, distribution, and type. McCool (17, p. 56) noted an interesting relationship between vegetal resistance and discharge or depth. As the discharge increases, the force exerted by the flowing water causes the vegetation to bend. When the vegetation is flattened to the channel bed, a portion of the channel cross section is freed to flow and the resistance decreases sharply. Test results for bermudagrass showed a nearly constant, high value of n for low flows, a rapidly decreasing n for medium flows where the grass was bending, and a fairly constant low n value for high flows when the grass was bent over.

The Manning Equation with constant n is applicable to the fully rough zone of turbulent flow. The Reynolds number is the usual criterion for identifying the fully turbulent regime. For sufficiently high Reynolds numbers, Manning's n is very nearly constant (2).

Gradually Varied Flow Applications

With increasing spatially varied or gradually varied flows, water runs in along the course. If the volume of added water is large compared to the volume of water flowing in the course, an appreciable portion of the energy loss is due to the turbulent mixing of the added water flowing in the channel (4).

Though Manning's n was originally used as a measure of watershed roughness for steady uniform flow, many experimenters have also employed it with unsteady flow problems. Favorable results have been obtained for many of these investigations. Other investigations have raised questions as to the applicability of n under these conditions.

Harbaugh (6) states that the employment of a constant value of Manning's n appears to yield satisfactory results even in unsteady flow if the range of depths is not large, and if the depth of flow is large relative to the size of roughness. Comparing two channels, all other factors being equal, the lesser average depth gives the higher n value, owing to the roughness elements being a greater percentage of the depth (4). Thus, if Manning's n is used to express roughness, its value for a given surface subjected to spatially varied flow will decrease with increasing depth of flow. This behavior is confirmed by uniform flow experiments conducted for a range of discharges by Woo and Brater (26).

The results of Woo and Brater for uniform flow do not
include the force needed to accelerate the lateral inflow
or indicate the influence of added turbulence due to rain-
drop impact. Harbaugh (6) noted that factors affecting the
turbulence induced are size of raindrop, velocity of rain-
drop, intensity of rainfall, type of rainfall simulator,
and slope of the plane over which the spatially varied flow
occurs. He found that the coefficient of watershed rough-
ness was different for three different rainfall intensities.
Higher coefficients of roughness were calculated for the
higher rainfall intensities. Parsons (18) obtained an
extra depth for rainfall-disturbed flow compared to uniform
flow, which he credited to spray-drop impact. He used Type
F nozzles operating at 35 pounds per square inch spraying
onto a small initial flow in an ungrassed channel. The
excess depth ranged from 8 to 28 percent of the average
depth, averaging 17 percent. There was no consistent vari-
ation in relative depth increase in relation to variation
in slope, flow rate, or spray rate. Parsons suggested that
different slope and discharge ranges may be affected by
different roughness characteristics of the bed.

Keulegan (14) states that although direct resistance
of the falling rain is usually small, the perturbing effect
may be appreciable, since the entering rain accentuates the
velocity gradient near the bottom. Upon the cessation of
rainfall and the resultant removal of its retardance effect,
Izzard (10) observed increases in channel outflow as great

as 15 percent. His tests were run on a smooth asphalt-
mastic surface, a crushed slate roofing paper, and a dense
bluegrass turf sod. Woo and Brater (26) noted that the
outflow increases occur primarily for flows which are of an
intermediate type between the laminar and turbulent regimes.
They suggested the possibility that the falling rain causes
flows which would otherwise be laminar to become turbulent.

Robertson (23) concluded that for steep, rough sur-
faces, the effect of the raindrop momentum and the turbu-
lence induced by the drops is small compared with the drag
force of the surface. He surmised that the resistance
coefficient determined from uniform flow tests could be
used to evaluate the drag force for spatially varied flow
conditions on steep, rough surfaces. Robertson's con-
clusions were based on experiments with a five percent slope,
concrete channel with pea gravel attached to the bottom.

Ragan (19) found that the roughness coefficients de-
termined for some steady state spatially varied flows were
essentially the same as those obtained under uniform flow
conditions for the same discharge. This conclusion was for
low magnitude lateral inflows, or lateral inflows super-
imposed on a base flow to a maximum ratio of one part
lateral to one part base flow. The similarity between
spatially varied and uniform flow was not as good when
either the magnitude of the lateral inflow was increased
or the base flow decreased. The steady state roughness
coefficients were obtained with a minimum of impact from the

lateral inflows. Higher values of the roughness coefficient probably would have resulted if the lateral inflow jets had been allowed to impinge directly on the water surface.

Water Surface Prediction Equations

Unsteady State General Equations

In unsteady spatially varied flow, velocity varies with time and position. Keulegan (14) utilized a rigorous mathematical analysis to derive the equation of continuity and the dynamic equation of motion for spatially varied flow. The continuity equation is:

$$VY = \int_0^x q \, dx - \int_0^x \frac{\partial Y}{\partial t} \, dx + V_o Y_o \qquad (2)$$

The dynamic equation is:

$$\left(\frac{dV}{dt} + \frac{V \partial V}{\partial x}\right) = g\left(S_o - \frac{\partial Y}{\partial x}\right) - \left(\frac{\lambda}{2}\right)\left(\frac{V^2}{Y}\right) - \frac{qV}{Y} \qquad (3)$$

where

Y_o = depth of flow at $x = o$

Y = depth of flow

t = time

x = distance from some reference point

q = discharge per unit width

S_o = slope of the plane

g = acceleration due to gravity

λ = coefficient of friction

Simultaneous solution of these two equations results in an estimate of depth and velocity for a specified location at

a specified time. Their solution can only be approximated.
The computation by finite difference is extremely tedious
and laborious. The attraction of these equations is that
they are analytically based. High speed computers reduce
the labor and make finite difference solution feasible.
However, the proper friction factor is necessary for correct
solution.

Steady State General Equations

When the change in velocity per change in time is zero,
steady state gradually varied flow is achieved. Steady
state gradually varied flow is amenable to solution by two
approaches: the law of energy conservation and the law of
momentum conservation (24). According to Chow (4) the
energy and momentum concepts produce practically identical
results for gradually varied flow. On page 51, Chow states:

> . . . The inherent distinction between the
> two principles lies in the fact that energy is
> a scalar quantity whereas momentum is a vector
> quantity; also, the energy equation contains a
> term for internal losses, whereas the momentum
> equation contains a term for external resistance.

The dynamic equation for steady state spatially varied
flows is (15):

$$- \frac{\partial Y}{\partial x} + S_o - S_f = \frac{V}{g} \frac{\partial V}{\partial x} + \frac{qV}{ga} \tag{4}$$

where a is the cross sectional area of flow per foot of
width. King and Brater (15) derive the steady state
continuity equation as follows:

$$aV - \frac{\partial a}{\partial t} \, dx + qdx = (V + \frac{\partial V}{\partial x} \, dx)(a + \frac{\partial a}{\partial x} \, dx)$$

Upon cancelling terms, eliminating higher order differentials, dividing by dx, noting that a equals Y, and noting that ∂a equals ∂Y, King and Brater found the steady spatially varied flow continuity equation for a unit width to be:

$$q = V \frac{\partial Y}{\partial x} + Y \frac{\partial V}{\partial x} \tag{5}$$

Increasing Steady State Energy Equation

The Bernoulli energy equation can be written for gradually varied flow in open channels as (4):

$$Z_1 + Y_1 \cos \theta + \alpha_1 \frac{V_1^2}{2g} = Z_2 + Y_2 \cos \theta + \alpha_2 \frac{V_2^2}{2g} + H_{fx}$$

For channel cross-sections 1 and 2, Z is the bottom elevation, Y is the depth perpendicular to the bottom, θ is the bottom angle of inclination, and V is the mean velocity. Also, the Coriolis velocity coefficient is α, H_{fx} denotes the internal energy dissipation in the reach of length x and g is the acceleration of gravity. Assuming that α_1 and α_2 are equal to unity and that θ is small, the energy equation can be rewritten:

$$Z_1 + Y_1 + \frac{V_1^2}{2g} = Z_2 + Y_2 + \frac{V_2^2}{2g} + H_{fx} \tag{6}$$

For an increasing steady spatially varied flow, assuming a parabolic water surface, H_{fx} equals $\overline{S}_{fx} \, x$,

where $\overline{S}_{fx}$ is the effective energy slope from station 1 to station 2. Assuming S_f to be the energy slope at station 1 computed by means of the Manning equation, and assuming S_{fx} to be the energy slope at any point x distance from station 1, (x = o), the equations for S_{fx} and $\overline{S}_{fx}$ are:

$$S_{fx} = S_f \left[\frac{Q_1 + (\phi)(x)}{Q_1} \right]^2$$

and,

$$\overline{S}_{fx} = \frac{\int_o^x S_{fx}\ dx}{x}$$

where ϕ equals the flow added per unit x increment. Substituting the equivalent of S_f from the Manning equation, the equation for $\overline{S}_{fx}$ becomes:

$$\overline{S}_{fx} = \frac{n^2\ Q_1^2}{(1.486)^2\ (A_1)^2\ (R_1)^{4/3}\ (x)} \cdot$$
$$\cdot \left[\int_o^x \left(\frac{Q_1^2 + 2\ Q_1\ (\phi)(x) + (\phi)^2 (x)^2}{Q_1^2} \right) dx \right]$$

Integrating this equation yields:

$$\overline{S}_{fx} = \frac{n^2}{(2.2086)\ (A_1)^2\ (R_1)^{4/3}\ (x)} \cdot$$
$$\cdot \left[Q_1^2\ x + Q_1\ (\phi)\ (x^2) + \frac{(\phi)^2\ (x)^3}{3} \right]_o^x$$

The equation for H_{fx} can now be written:

$$H_{fx} = (\overline{S}_{fx})(x) = \frac{n^2}{(2.2086)(A_1)^2(R_1)^{4/3}} \cdot$$

$$\cdot \left[Q_1^2 x + Q_1 (\phi)(x)^2 + \frac{(\phi)^2(x)^3}{3} \right] \qquad (7)$$

The energy equation can be written as:

$$\Delta Y = -\Delta H_{Vx} + \Delta Z - H_{fx} \qquad (8)$$

where ΔZ equals the bottom slope times x or $Z_1 - Z_2$, and ΔH_{Vx} equals the velocity head change, $H_{V_2} - H_{V_1}$. The equations for H_{V_1} and H_{V_2} can be written:

$$H_{V_1} = \frac{V_1^2}{(2)(g)} = \frac{Q_1^2}{A_1^2(2)(g)}$$

and,

$$H_{V_2} = \frac{Q_2^2}{A_2^2(2)(g)} =$$

$$\left[Q_1^2 \left(\frac{Q_1^2 + 2(Q_1)(\phi)(x) + ((\phi)(x))^2}{Q_1^2(2)g A_2} \right) \right]$$

Upon simplification the equation for $-\Delta H_{Vx}$ can be written:

$$-\Delta H_{Vx} = \frac{Q_1^2}{(2)(g)(A_1)^2} \left[-\frac{2(\phi)(x)}{Q_1} - \frac{((\phi)(x))^2}{Q_1^2} \right]$$

Now the energy equation can be expressed in computational form as:

$$\Delta Y = \frac{Q_1^2}{2gA_1^2}\left[-\frac{(2)(\phi)(x)}{Q_1} - \frac{((\phi)(x))^2}{Q_1^2}\right] + S_o x -$$

$$\left[\frac{n^2}{(2.2086)(A_1)^2(R_1)^{4/3}}\right]\left[(Q_1)^2(x) + (Q_1)\right.$$

$$\left.(\phi)(x)^2 + \frac{(\phi)^2(x)^3}{3}\right] \tag{9}$$

Henderson (7) suggested a step method of solution for the energy equation for which he assumed the water surface linear so that the average of the friction slopes at the ends of the section under consideration is the average friction slope. If two stations are separated by a distance ΔX, the energy equation can be written as follows:

$$E_2 - E_1 = (S_o - .5\, S_{f1} - .5\, S_{f2})\, \Delta x \tag{10}$$

where E refers to specific energy.

Increasing Steady State Momentum Equation

If the volume of added water is large compared to the volume of channel flow, the impact or mixing losses will be appreciable. The momentum equation for predicting the surface profile for increasing spatially varied flow takes into consideration the effect of the impact loss (4). If the stations are again labeled (upstream) 1 and (downstream) 2, the momentum passing sections 1 and 2, respectively, is:

$$\frac{w}{g}(Q_1)(V_1)$$

and

$$\frac{w}{g} (Q_1 + dQ) \ (V_1 + dV)$$

where w is the unit weight of water, Q_1 is the flow at
station 1, V_1 is the velocity at station 1, and dQ is the
added discharge between the two stations. The momentum
change in the section is:

$$\frac{w}{g} \left[Q_1 \ dV + (V_1 + dV) \ dQ \right]$$

If W is the weight of the water between the stations,
the component of W in the direction of flow, the gravity
force , is (W sin θ), where θ is the angle the plane makes
with the horizontal. The frictional or shear force along
the channel wall is equivalent to the pressure due to
friction head multiplied by the average area, or:

$$F_f = w \ (A_1 + 1/2 \ dA) \ S_f \ dx$$

The resultant hydrostatic pressure acting on the volume of
water between stations 1 and 2 is:

$$P_1 - P_2 = - wA \ dY$$

Equating the momentum change of the water volume to
all external forces acting on the body:

$$\frac{w}{g} \left[QdV + (V + dV) \ dQ \right] = P_1 - P_2 + W \sin θ - F_f$$

Considering the differentials as finite increments yields the following equation:

$$\frac{w}{g} \left[Q\Delta V + (V + \Delta V) \Delta Q \right] = - (w) (\overline{A}) (\Delta Y) + (w)(S_o)$$

$$(\overline{A}) (\Delta x) - (w) (S_f) (\overline{A}) (\Delta x)$$

where $\overline{A}$ is the average area. Since the discharge varies with the finite increment of the channel length, the average area may be calculated as:

$$\overline{A} = (Q_1 + Q_2)/(V_1 + V_2)$$

Assuming $Q = Q_1$ and $V + \Delta V = V_2$, and simplifying:

$$\Delta Y = - \frac{Q_1 (V_1 + V_2)}{g (Q_1 + Q_2)} \left[\Delta V + \frac{(V_2) (\Delta Q)}{Q_1} \right] +$$

$$(S_o - S_f) (\Delta x) \tag{11}$$

This equation can be used to calculate the change in depth for steady spatially varied flow with increasing discharge, if Q_1, ΔQ, and Y at some point along the channel are known. On the right-hand side of the equation, the first term represents the impact loss and S_f times x represents friction loss (4).

Previous Solutions

Ragan (19) set up computer programs for the solution of the partial differential equations of unsteady spatially varied flow. The programs were designed to use the roughness coefficients obtained from steady state spatially varied flow studies. So that the influence of the roughness

coefficient could be determined, the programs were arranged
to return to their initial conditions following a run,
change the Manning's n by a given percentage, and repeat
the computation using the new roughness coefficient. In
some runs, especially those with no base flow, an error
of .011 feet in the depth reading could change the n value
by 5 percent. The numerical solution was found to be quite
sensitive to errors in the value of the roughness coeffic-
ient.

In 1963, Brakensiek (1) utilized an IBM 1620 and an
implicit technique to study the feasibility of using a
numeric method for routing floods through natural channels.
Because of storage and speed limitations, he reduced the
momentum equation to $dY = (S_o - S_f)\, dx$. This equation
neglects the impact term. If the entering rainfall volume
is small compared to the channel flow volume, neglecting
the impact term should not substantially alter the solution
for field problems.

In 1964 McCool (17) conducted increasing spatially
varied flow tests at 5, 10, 20, 30, and 40 cubic feet per
second to provide a comparison for water surface profile
predictions made using theoretical equations. He used
resistance and velocity distribution characteristics as
input for computer solution of those equations. When
suitable Boussinesq coefficient and resistance relationships
were used, McCool found that the increasing steady state
equation developed from the momentum concept gave a good

prediction of water surface profile. The experimental facility employed was a V-shaped bermudagrass-lined channel. The channel was 410 feet long with .001 bottom slope and free outfall at the outlet.

Regimes of Flow

Among the regimes of flow commonly encountered in open channel flow are laminar, mixed laminar and turbulent, and fully turbulent. A fourth regime shall be referred to as constant-velocity flow.

General equations for these flow regimes are:

Constant-velocity	$Y = (K_{cV})\ (Q)$	(12)
Laminar	$Y = (K_{L})\ (Q)^{0.33}$	(13)
Mixed	$Y = (K_{M})\ (Q)^{M}$, M variable	(14)
Turbulent	$Y = (K_{T})\ (Q)^{0.6}$	(15)

Constant-Velocity Flow

According to Horton (9) overland flow may be so sub-divided by grass or vegetal matter as to produce a condition where the velocity of the flow is sensibly constant, i. e. $Y = (K_{cV})\ (Q)^{1.0}$. This equation is interestingly similar to that of Darcy's law of artificial filtration through a uniform, unstratified soil, which is expressed as $Q = (K_{p})$ (A) (i). Here K_{p} is the coefficient of permeability and i is the hydraulic gradient.

Laminar Flow

When proper conditions are fulfilled, the flow of a fluid is of a relatively simple type called laminar or streamline. The fluid moves in parallel layers with no cross currents. Flow will be laminar when the velocity is not too great and the geometry of the channel bed is not such as to cause the lines of flow to change direction too abruptly. Low sheet flows at very small depths have been shown by Horton, Leach, and Van Vliet (8) to be laminar or viscous.

The Reynolds number is usually used as a criterion for determining whether flow is laminar or turbulent. Ree (22) stated that the Reynolds number for the point of separation between laminar and turbulent flow has been found to be between 300 and 3000.

Mixed Flow

Parsons (18) advocated the idea that other factors besides the bulk Reynolds number apparently influence the upper limit of viscous type flow, and that the change is from laminar to an intermediate type flow rather than to strictly turbulent flow. He found the point of change well within the overland flow range.

Referring to this mixed flow or transition regime, McCool (17, page 46) stated:

> . . . An increase in velocity will eventually lead to turbulent flow past a smooth boundary or turbulent flow with a laminar boundary layer. The boundary roughness does not materially affect the

resistance in this partially turbulent flow, be-
cause the roughness elements are shielded by the
boundary layer. As the velocity is increased, a
point will eventually be reached where the laminar
boundary layer is thinned sufficiently that the
boundary roughness becomes exposed to the direct
action of the moving fluid, and the flow goes into
the fully turbulent mode.

Turbulent Flow

In contrast to laminar flow, turbulent flow is very

irregular. In the turbulent regime resistance depends upon

the roughness of the boundary, and is independent of

viscosity (17). Turbulent flow is characterized by

pulsatory cross-current velocities. Both the magnitude and

the direction of the instantaneous velocity are functions

of time as well as space. One result of the cross-current

velocities of turbulent flow is the formation of a more

uniform velocity distribution (15). One of the most im-

portant practical differences between laminar and turbulent

flow is the much greater energy loss in turbulent flow.

According to Wright and Lemon (28), the irregular

feature of turbulence makes it impossible to describe the

motion in all details; however, certain aspects of turbulent

motion can be described by means of probability and mean

quantities. The shearing stress between two fluid layers

in highly turbulent flow is not due to molecular friction,

but rather to momentum transfer by motions of macroscopic

bodies of fluid normal to the main direction of flow.

CHAPTER III

EXPERIMENTAL EQUIPMENT

The Channel

The channel and all associated equipment were located
indoors. A 44-foot long 18 - by 7½-inch steel WF beam was
supported on its side to form a variable slope rectangular
flume. The bottom was lined with PERMA-GRASS, an artificial
grass which was assumed to simulate a close growing mat
type grass as bermudagrass. The sides of the channel were
lined with half-inch masonite with a finished smooth sur-
face. The masonite was cut at a 45-degree angle at the
bottom in order to stop channeling in an open space between
the channel edge and the grass. The channel width inside
the masonite was 1.325 feet or almost 16 inches. The
channel slope was adjusted by variable height supports.
These were pipe stands with holes at calculated intervals
for adjusting the slope. A general view of the experimental
channel is shown in Figure 1.

The Water Supply Systems

Two water supply systems were used, a uniform flow
system and a sprinkler or rainfall system. Two Bell and

Figure 1. General View of the Experimental Channel.

Cossett 1531 Type B pumps were used to withdraw water from a 9- by 5- by 5-foot sump. The intake for the sprinkler system had a 9-inch cubic steel frame covered with 16 mesh screen. Also a 20 mesh on-the-line strainer was placed in the sprinkler line to keep the nozzle heads and filters from clogging. Both systems had 1¼ inch galvanized pipes running from the pumps to the upstream end of the channel. These pipes were supported by a large wooden frame.

The uniform flow system discharged water vertically and directly into the upper end of the channel. The turbulence of the entering flow was decreased by forcing the water to flow over a 2- by 2-inch wooden block and through 8 and 16 mesh screens.

The sprinkler system had a 3/4-inch aluminum pipe running about 3 inches to the side of the channel. This pipe was attached by means of thick sheet metal bent at near right angles. One side of the angle was clamped by a C clamp to the side of the channel; the 3/4-inch pipe was supported by the other side of the angle. Drilled in the latter side of the angle was a hole over which a locknut was tightened onto the top of a special Tee-Jet saddle clamp, nozzle body assembly. The sheet metal support, saddle clamp, nozzle, and nozzle assembly are illustrated in Figure 2. At each of the support areas, a hinge for a nozzle cover was installed. The nozzle cover was light gage sheet metal bent in the approximate shape of a U. One man could instantaneously start or stop the simulated
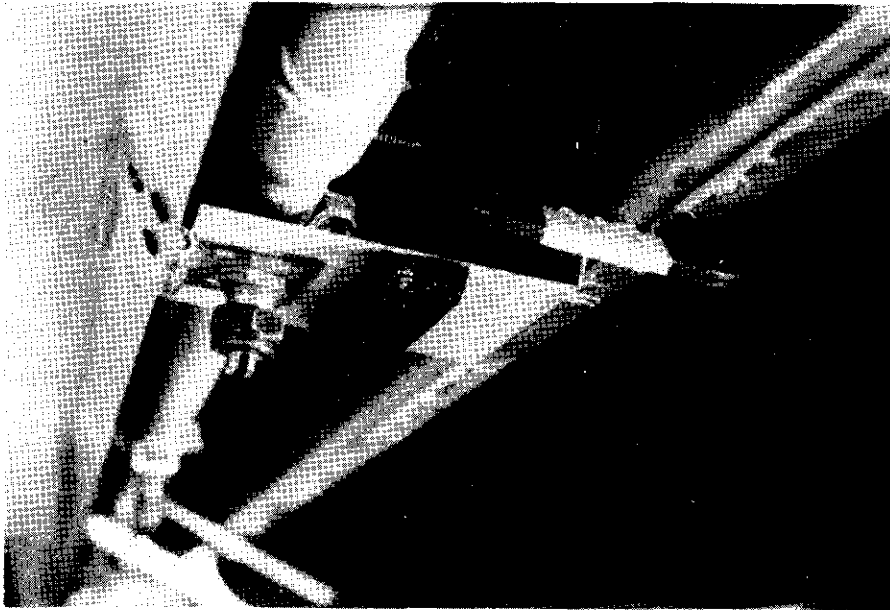
rainfall by rotating the cover. Due to the sensitivity of other electronic measuring equipment, rubber pads were placed at several locations to dampen channel vibrations caused by opening and closing the sprinkler cover.

The nozzles used were brass Tee-Jet 8002E and 8008 fan types, filtered by 50 mesh screens. The 8002E nozzles supplied approximately 1.3 and 2.6 inches per hour at 1.5 and 3.0-foot spacings, respectively, while the 8008 group at similar spacings supplied about 4 and 8 inches per hour. Blank nozzles were used at every other sprinkler station to obtain the 3.0-foot spacings. The sprinkler system was operated at a pressure near 4 pounds per square inch. Marsh Pressure gages, 0 to 15 pounds per square inch, were installed at each end of the 3/4-inch pipe. The gages had graduations of ¼ pound per square inch.

In an attempt to achieve uniformity of ejection angle for the nozzles, a line was cut along the pipe with a lathe. The holes for the nozzle inserts were drilled along this line. The holes were drilled slightly oversize to allow for some angle adjustment. The rubber gaskets of the saddle clamp, nozzle body assembly kept leakage near zero. The special collection device shown in Figure 3 was used to adjust nozzle orientation for uniform application. This device consisted of a sloped corrugated metal surface set on a wooden base, and a wooden test tube holder with a test tube at the lower end of each corrugation. A graduated
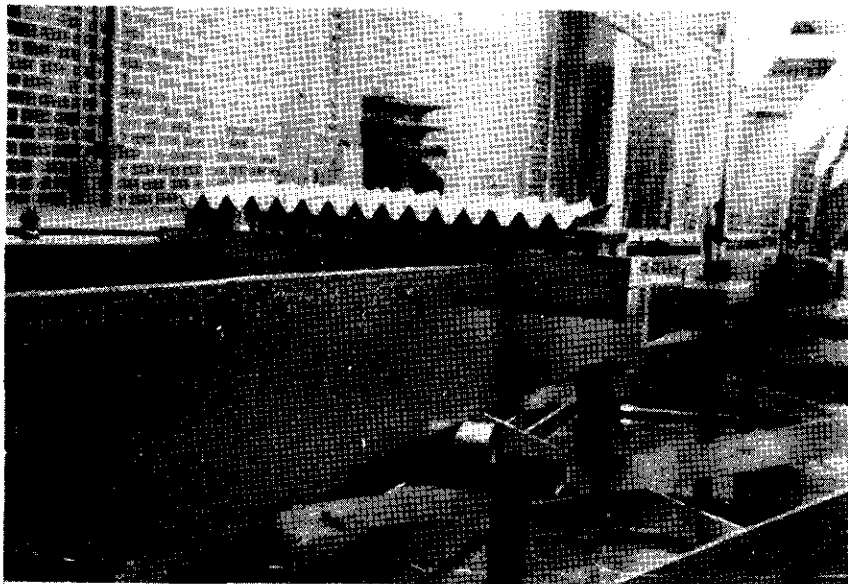
Figure 3.   The Special Collection Device
            Used to Check the Relative
            Rainfall Uniformity Across
            the Channel.

cylinder was used to measure the relative amounts of water collected by the surface and tubes across the channel.

Flow Measuring Equipment

A 0.6 H.S. flume of about 34 gallons per minute capacity was used to measure total outflow at the lower end of the channel. The discharging water had to fall about 1¼ feet through a 3-inch pipe bent in an approximate S shape. This pipe was filled with screen and 3/4-inch white plastic balls to slow the fall velocity. The water discharged vertically about ½ inches above the flume bottom. Two screens of 10 and 16 mesh were used to dissipate the turbulence of the flow in the flume. An adjustable height trough was utilized in the return of water to the sump from the H.S. flume outlet.

The H.S. flume stilling well water level could be measured at any desired time by means of a point gage. A continuous record of the head in the H.S. flume was obtained with a Belfort Friez FW-1 Recorder. The chart cylinder of the recorder was driven by an a.c. capacitance motor at a speed of one revolution per hour. The H.S. flume and the water level recorder are shown in Figure 4.

The discharge for the uniform flow system pump was measured by a 1-inch, A-type Badger flow meter. The total discharge rate for low flows was also determined by collecting the outflow in a bucket for a certain time period. Laboratory scales were used to obtain the weight of the
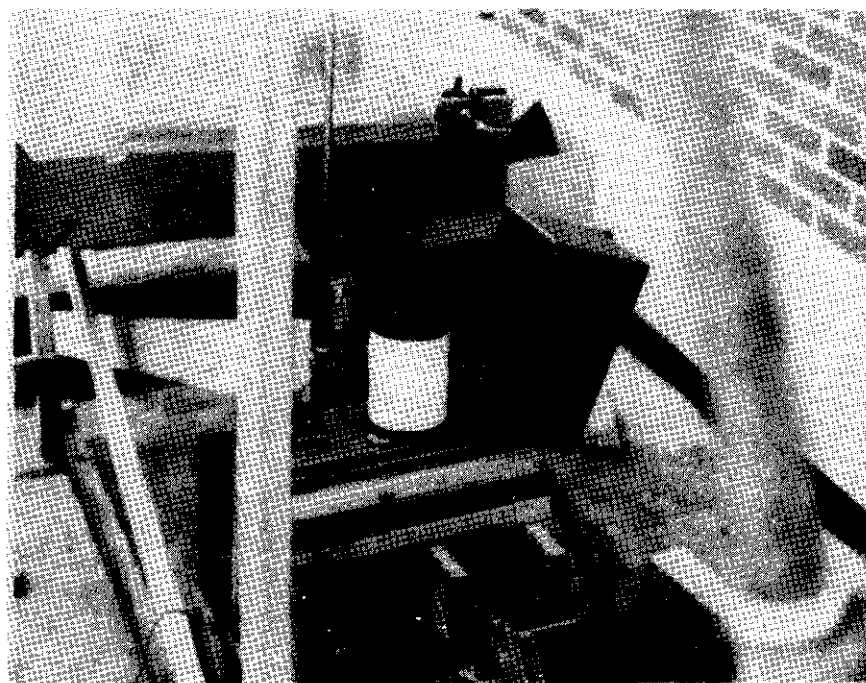
Figure 4.   The 0.6 H.S. Flume and Water Lev-
el Recorder Used for Discharge
Measurement.

water and the bucket.

Depth Measuring Equipment

Four stilling wells and point gages were installed along the channel. These stations were located about 11, 21, 31, and 40 feet down the channel from the upstream end. At each station brass plugs with holes of about .07 inches diameter were used as piezometers to measure the flow depth. The brass plugs were set level with the bottom of the channel and protruded from the lower side of the steel beam. Three plugs were placed in line across the channel. Their location was such that each piezometer measured an equal area across the channel. Rubber and brass tubing connected the piezometers with the stilling wells.

A Physiological Pressure Transducer, Hewlett-Packard Model Number 268B, was used in conjunction with each stilling well to give a continuous depth record. This arrangement is illustrated in Figure 5. The transducers were mounted on stands glued to the floor to prevent ex-cessive vibration and movement. These stands had steel bases with galvanized steel pipes welded to the base; polyvinyl chloride tubing was fitted over the pipes to support the transducers and to allow height adjustment. The four transducers were wired into the two Sanborn Model 321 Dual Channel Carrier Amplifier-Recorders which are shown in Figure 6. A Stabiline Voltage Regulator, Series 1414, Type IE 51005, kept the input voltage to the Sanborn
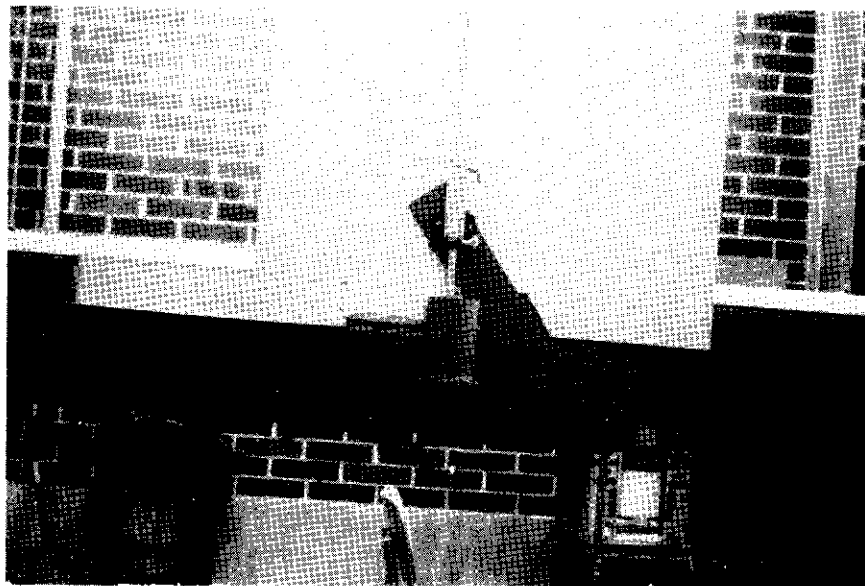
Figure 5.   Side View of a Stilling Well With
Point Gage and Transducer.
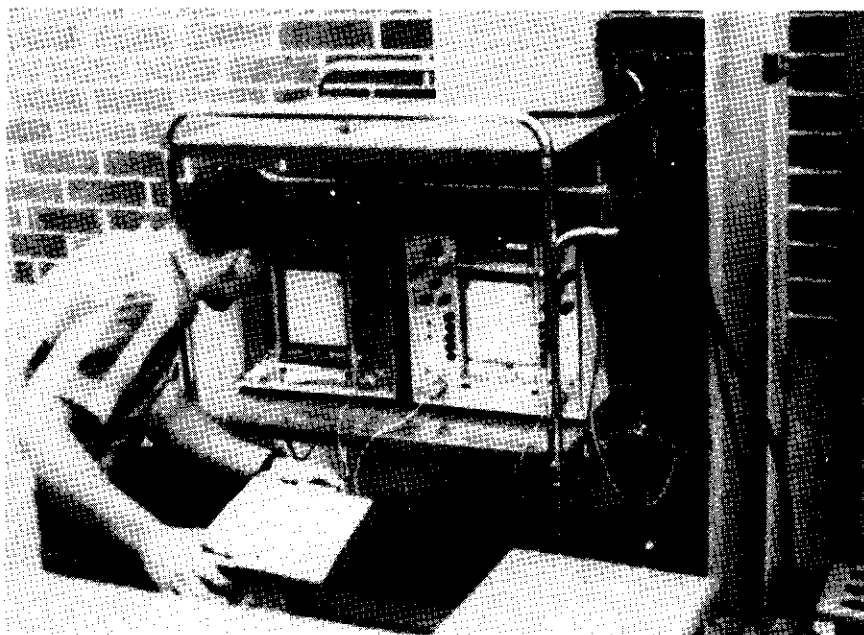
Figure 6.   The Two Sanborn Dual Channel
Amplifier-Recorders.

recorders constant. The transducers were so sensitive that even drops of water falling on the transducer wire caused a wide, nebulous line on the Sanborn recorder paper. Shields made from sheet metal and plastic sheets were set up at each station to keep water off the transducers, point gages, and reader and to prevent the fall of water into the stilling wells.

Gage Zero Equipment

A Zeiss precision level was used to find the elevation of the central brass plugs at each station along the channel. A point gage with a blunt end was utilized as a rod gage. Shims were employed in adjusting the channel slope. The precision level was also utilized in obtaining gage zeros for the point gages. The gage zero for the H.S. flume was found with the aid of a Keuffel and Esser dumpy level.

CHAPTER IV

METHODS AND PROCEDURE

Preliminary Investigation

A preliminary investigation of nozzle orientation and spacing was conducted in order to obtain the desired rainfall rates and relative uniformity. The first type nozzle tested was the spraying system ¼HH 14W. These sprinklers were spaced at 52.5-inch intervals along the channel, and operated at pressures from 5 to 20 pounds per square inch in an effort to achieve different intensities of rainfall. The height of the nozzles, which ejected water vertically down on the channel, was varied from 22 to 32 inches in attempting to obtain overlapping of the spray from one sprinkler to the next. Varying the operating pressure did not change the intensity as much as desired, but changed the rain impact velocity quite markedly. The nozzle height adjustment did not yield overlapping of spray fringes.

A spray test rig for determining uniformity and volume of runoff was utilized in testing several other nozzles. Tee-Jet 8002E fan type nozzles spraying downward were evaluated for width and breadth of pattern associated with various combinations of pressure and height of nozzle.

Tee-Jet 650067 nozzles were tested spraying downward at high pressure. Next several nozzles were evaluated for upward discharge. The upward ejection pattern of Tee-Jet 8008 fan type nozzles is shown in Figure 7. Tee-Jet 8002E and 8008 nozzles were chosen since they produced most nearly the desired intensity and pattern of fall. The approximate single 8008 nozzle spray pattern is illustrated in Figure 8.

Drop Size Determination

The 8002E and 8008 nozzle drop sizes were determined, approximately, by a photographic technique. The drops were photographed in a relatively narrow focal field. A scale graduated in hundredths of an inch was photographed in the same field. This picture was then cut along the edge of the scale. Approximate drop diameters were measured by laying the scale over the pictures of the drops, as illustrated in Figure 9. Relative volumes of various groups of drop sizes were compared to the total volume of the drops observed. The total number of drops observed was also separated into the number of drops in several ranges of drop sizes. The results of the drop size studies are presented in Figures 10, 11, and 12.

The maximum height of drop fall on the channel for the 8008 nozzle was about 5 feet, while the average was 4.25 feet. The maximum for the 8002E nozzle was about 4.25 feet, while the average was 3.25 feet. Neglecting air resistance,

Figure 7. Ejection Pattern of Tee-Jet 8008 Fan Type Nozzles.
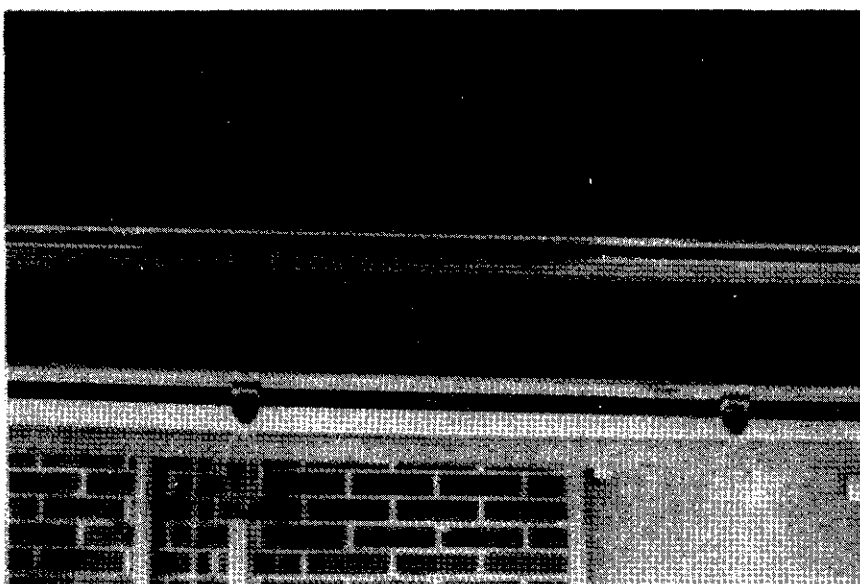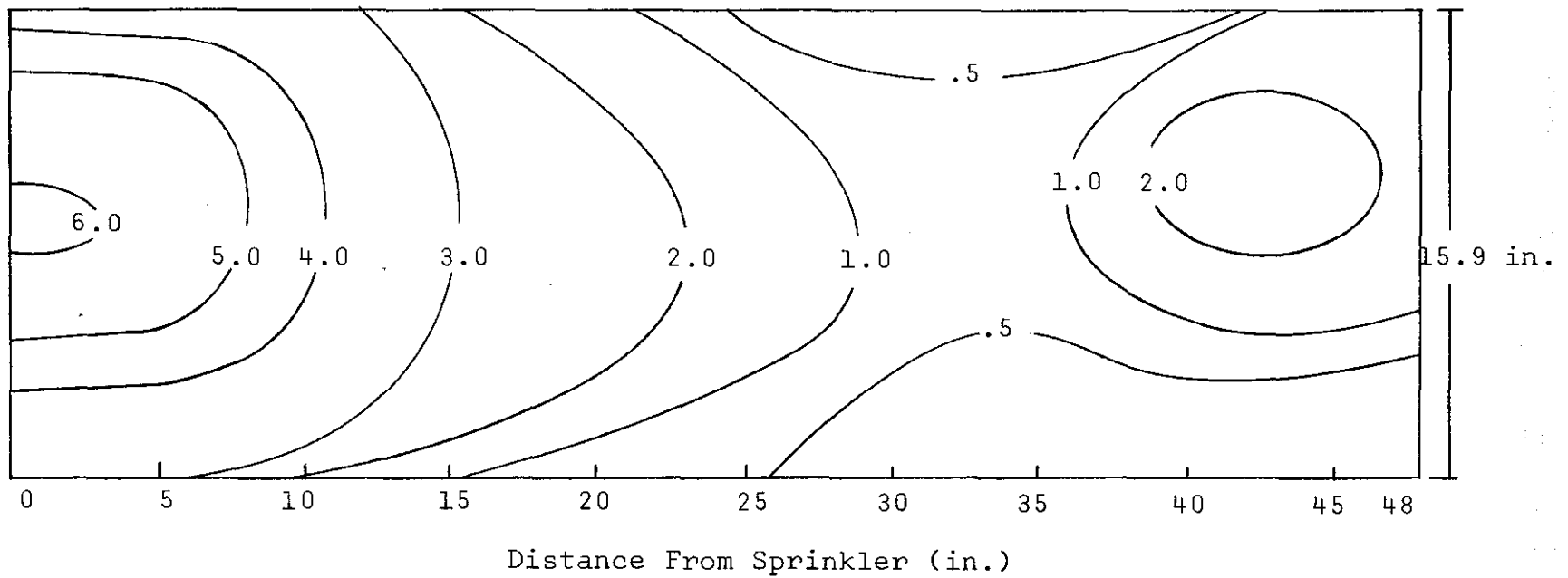
Figure 8. Approximate Single 8008 Nozzle Spray Pattern. The Lines Represent the Rainfall Intensity Identified by the Numbers.

Figure 9. Drop Size Determination Technique.
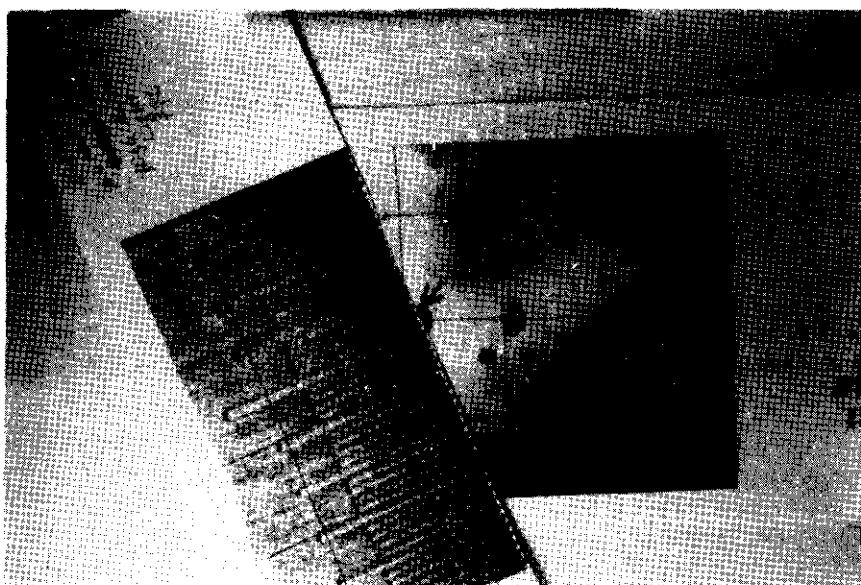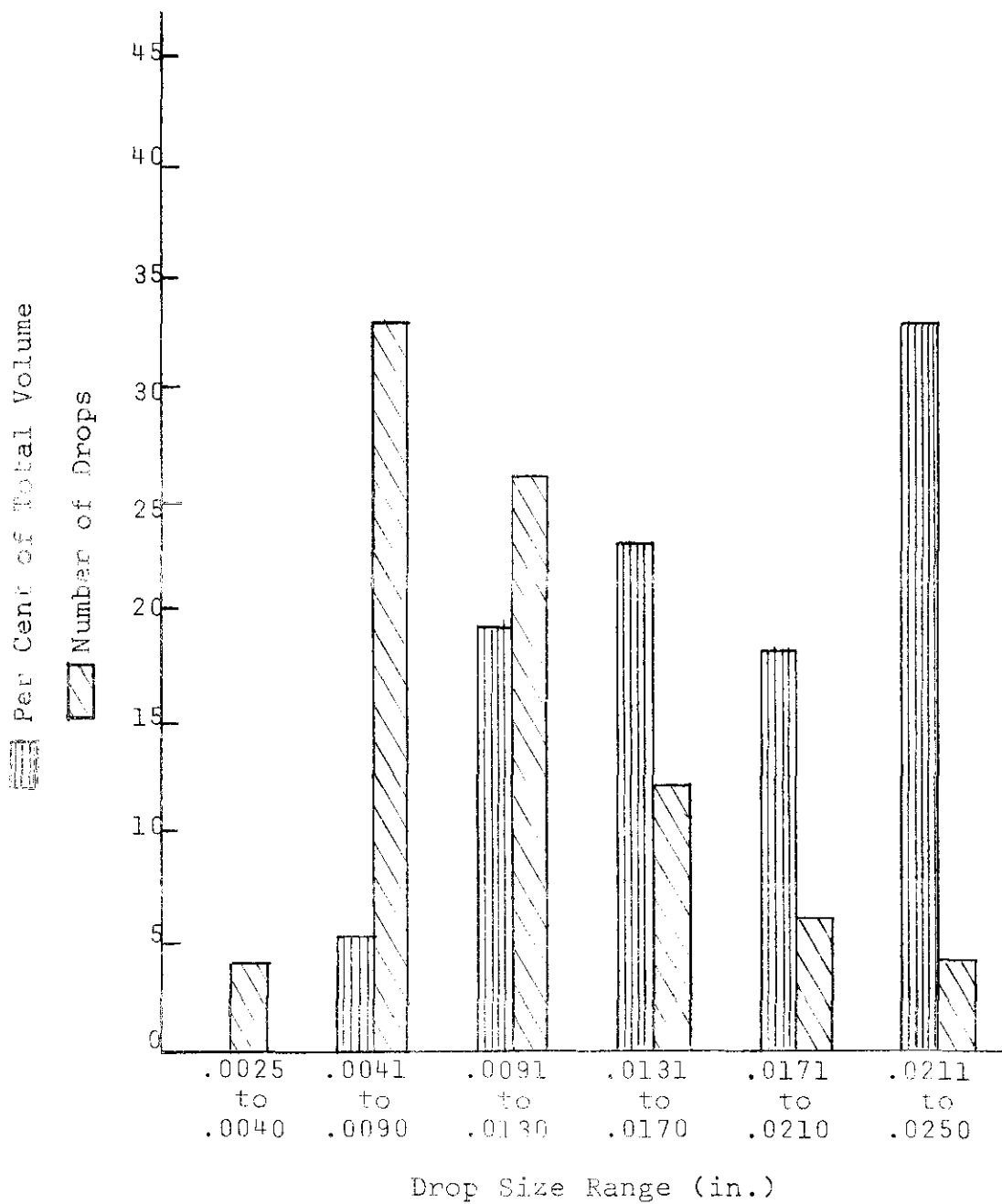
Figure 10.   Number of Drops and Per Cent of
             Total Drop Volume for Various
             Drop Size Ranges for 8002E
             Nozzles.
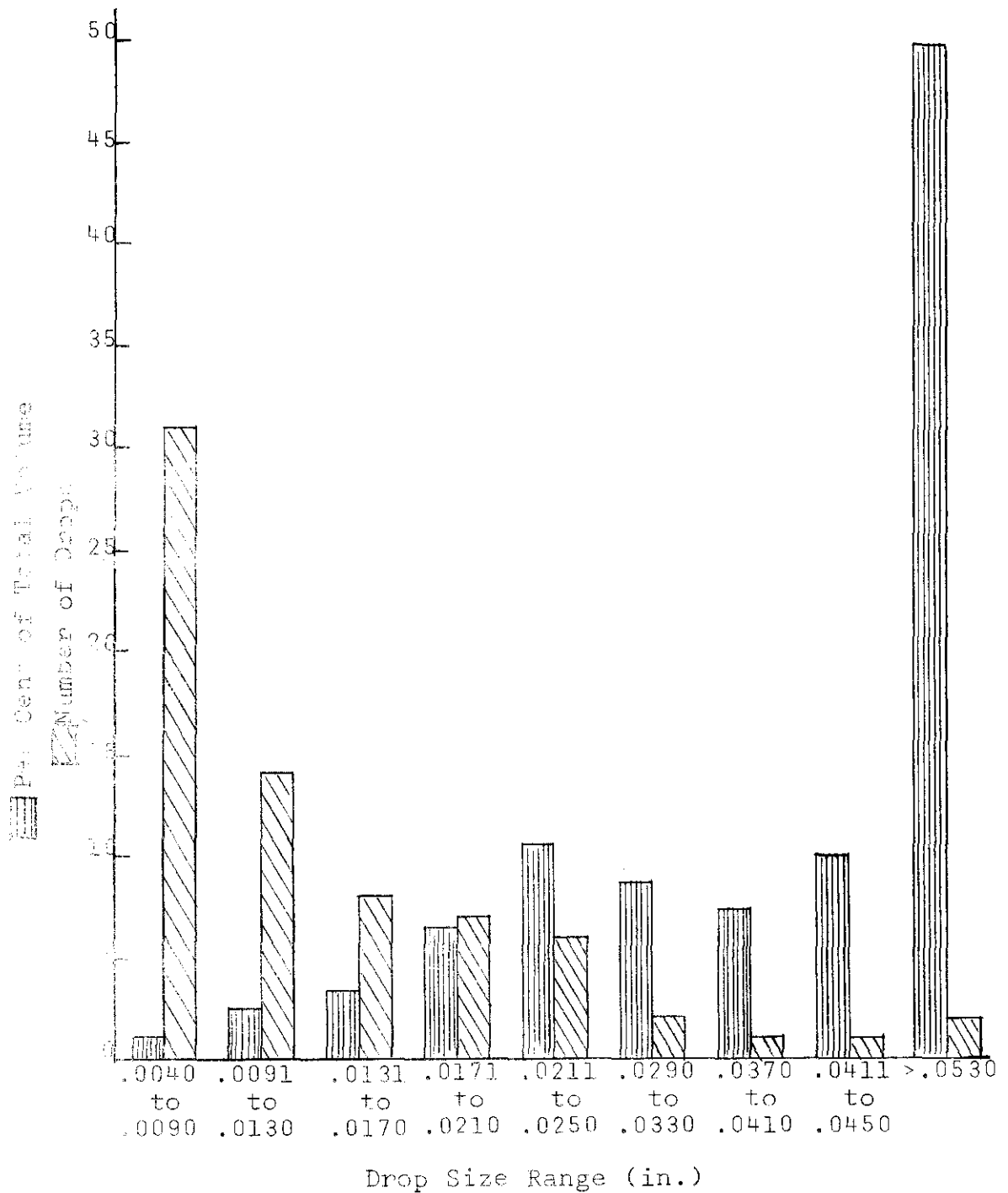
Figure 11. Number of Drops and Per Cent of Total Drop
Volume for Various Drop Size Ranges for
8008 Nozzles.
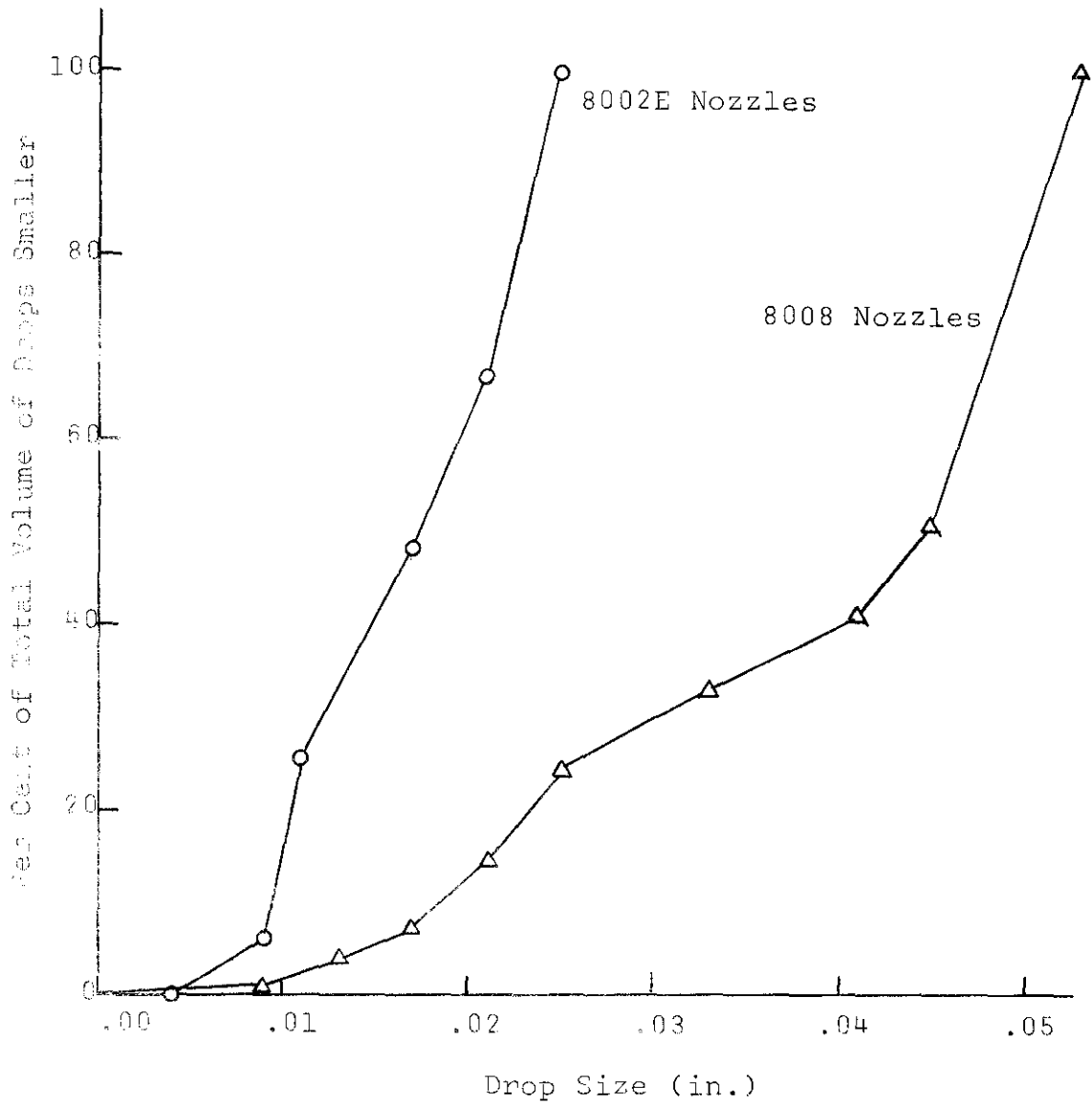
Figure 12. Drop Size Compared to Per Cent of Total Volume of Drops Smaller Than the Drop Size in Question.

the terminal velocity of a particle falling 5 feet is 17.94 feet per second and that for 3.25 feet is 14.46 feet per second. The effect of the drag due to air resistance on the various small sized particles is complex and was not calculated. The velocities as well as the raindrop diameters were not great enough to approximate those of real rainfall.

Slope Determination and Control

The elevation of the central brass plug at each station was referenced to a permanent bench mark. The relative elevations were determined using a Zeiss precision level and a blunt end point gage as a rod gage. During each original slope determination, shims were used in conjunction with the variable height channel supports to adjust the slope. The slope was checked every few days for channel settling or slipping on the supports; however, there was no noticeable change in elevation. Each time the slope was changed, the point gages were plumbed with a carpenter's level.

Gage Zeros

For the channel point gages, a gage zero was the elevation of the point gage tip when the zero mark on the point gage shaft coincided with the zero mark on the vernier scale. The Zeiss precision level was used to read the point gage standing on the bench mark (BM Rdg). The gage was then placed in its holder and adjusted to some

even reading on the level crosshair (Level Rdg). While the
point gage was so positioned, the gage vernier was read
(Vernier Rdg). The arbitrary elevation of the bench mark
was assumed as 10.000. The gage zero can be calculated as:

$$Gage\ Zero = (10.000 + Level\ Rdg) - (Vernier\ Rdg$$
$$+ BM\ Rdg)$$

For the H.S. flume a Keuffel and Esser dumpy level was
employed in gage zeroing operations. The gage zero was
actually the reading on the point gage vernier when its
point was at the flume lip elevation. This was convenient
since flume head calculations could be accomplished by one
subtraction. An instrument reading was taken with the
point gage on the flume lip (FL Rdg), as well as in-the-
holder observations similar to those of the channel point
gages. The H.S. flume gage zero can be calculated as:

$$H.S.\ Gage\ Zero = (FL\ Rdg) - (Level\ Rdg - Vernier$$
$$Rdg)$$

Rainfall Uniformity

Each time the rainfall intensity was varied, some
nozzle tips had to be installed or removed. The removal or
installation of nozzle tips resulted in some or all of them
not having the proper orientation to spray very uniformly
onto the channel. First the nozzles were adjusted visually
to approximate the proper orientation. Then the special

corrugated collection device described in the previous chapter was utilized in determining optimum sprinkler orientation. Adjustments were made by rotating the sprinkler pipe, individual sprinklers on the pipe, and the nozzles in the caps. The adjustment goal was to keep the maximum variation in uniformity across the channel at 50 percent of the largest amount collected from a single corrugation division. Maximum intensity was usually near the middle of the channel, with intensity decreasing toward the sides.

Transducer Calibration

Much difficulty was encountered in obtaining consistent readings from the transducer, Sanborn recorder combinations at first. However, after extensive adjustments they performed satisfactory. The line voltage varied sufficiently to cause some recorder variation. To remedy this, a stabiline voltage regulator was used and this kept the voltage constant within $\pm.1$ volts.

The stilling well level at each transducer was adjustable by adding or removing water with a battery filler for coarse and a medical syringe for fine adjustments. The point gage difference between two water levels was calculated and considered correct. The Sanborn difference was then checked against that of the point gages. Sanborn sensitivity was adjusted until the differences agreed within about .008 inches. The ability of the transducer, Sanborn combination to maintain calibration was established

by checks over a time period of several weeks. During
testing calibration was checked about twice a week.

Two of the major problems encountered with the trans-
ducer, Sanborn combination were drift and sensitivity to
mechanical vibration. In some cases where very small
depth changes were measured, the drift was larger than the
depth differences. Large trucks passing outside could be
detected on the recording. The pumps in the laboratory were
set on wooden blocks and rubber mounts to reduce the
transmitted vibration.

Testing Procedure

Uniform flow tests, illustrated in Figures 13 and 14
were conducted for each channel slope. Water was intro-
duced at the upstream end of the channel and after equilib-
rium was attained, the water level at each station was
measured with the point gages. The flow rate was measured
by one, two, or all of the following: flow meter, H.S.
flume, and weight per time. The flow meter and H.S. flume
had been calibrated previously. The weight per time flow
measurements were given precedence below 4.4 gallons per
minute; above this the average of all three methods was
accepted as more nearly correct. Weight per time flow
measurements were not usually taken above 10 gallons per
minute. For tests with discharges above 4.4 gallons per
minute, most of the flow measurements of the three methods
were within two or three percent of one another, though an

Figure 13.   Downstream View of Uniform Flow
of Six gpm at Three Per Cent
Channel Slope.
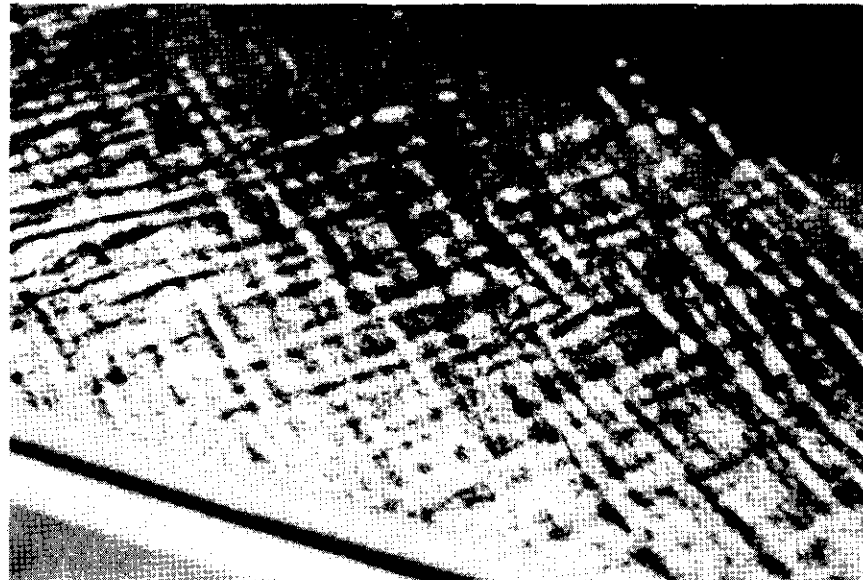
Figure 14.   The Water Surface for a Uni-
form Flow of 17 gpm at
Four Per Cent Channel
Slope.

occasional difference of four or five percent was noted.

Five spatially varied flow tests were run for each rainfall intensity at each slope. One of these had no base flow while the other four had a base flow. The base flow and depth were measured at equilibrium by the same methods as were used for uniform flow. The Sanborn recorders were set at an arbitrary zero at the base flow water surface. The Belfort recorder on the H.S. flume was turned on when the base flow was near equilibrium. Then the sprinkler cover was rotated back and simulated rainfall allowed to fall into the channel. Point gage and flow readings were taken after steady state conditions were reached. The sprinkler cover was then shut, stopping rainfall. Draw-down or recession depths were measured for most base flows which were less than four gallons per minute. Final base flow equilibrium depths were read, and all recorders were then turned off.

CHAPTER V

PRESENTATION AND ANALYSIS OF DATA

Uniform flow and increasing spatially varied flow experiments were conducted. Though steady state and unsteady state measurements were made for the spatially varied flows, only the steady state results are discussed in this thesis. The uniform flow tests were conducted to determine the hydraulic roughness in terms of Manning's n for turbulent, uniform flow. Another aim of the uniform flow tests was to determine the relationships between discharge and depth of flow in the non-turbulent regimes. The above relationships from the turbulent and non-turbulent regimes of uniform flow are used to predict the steady state increasing spatially varied flow water surface profiles.

The IBM 360 computer of the University was utilized in predicting the water surface profiles for the spatially varied turbulent regime by means of the energy and momentum equations. Simplified and complete forms of the momentum equation, Equation 11, were used to predict the water surface profile. Another simplified method of predicting the water surface profile is based on the assumption that the bottom slope is equal to the energy slope for the Manning Equation (assuming uniform flow). For this method,

50

Manning n values for uniform flow are assumed as applicable
to spatially varied flow.

Uniform Flow

Surface Tension Effects

Surface tension effects caused depth measurement diffi-
culties at very low flows, i.e. flows on the order of .1 or
.2 gallons per minute. Some of these low-flow depth
measurements indicated water levels below the bottom of the
channel. The brass plugs in the bottom of the channel had
holes of about .07 inches diameter. The capillary action of
these tubes caused the water level in the stilling well at
zero flow to register about .008 feet below the physical
bottom of the channel. When a glycerol wetting agent was
added so that surface tension was lowered from about 73 to
29 dynes per centimeter, the level in the stilling well at
zero flow was nearly the same as the channel bottom eleva-
tion. Thus, surface tension effects may have distorted some
of the very low depth readings in both uniform and spatially
varied flows.

Constant-Velocity Flow

The relative density of the grass stems is illustrated
in the views of PERMA-GRASS presented in Figures 15 and 16.
The grass occupies much of the cross-sectional flow area at
low flows. Surface tension and capillary effects are also
great. Observations were made where the flow was 1/4-inch
deep and where the internal regions of the round grass tufts
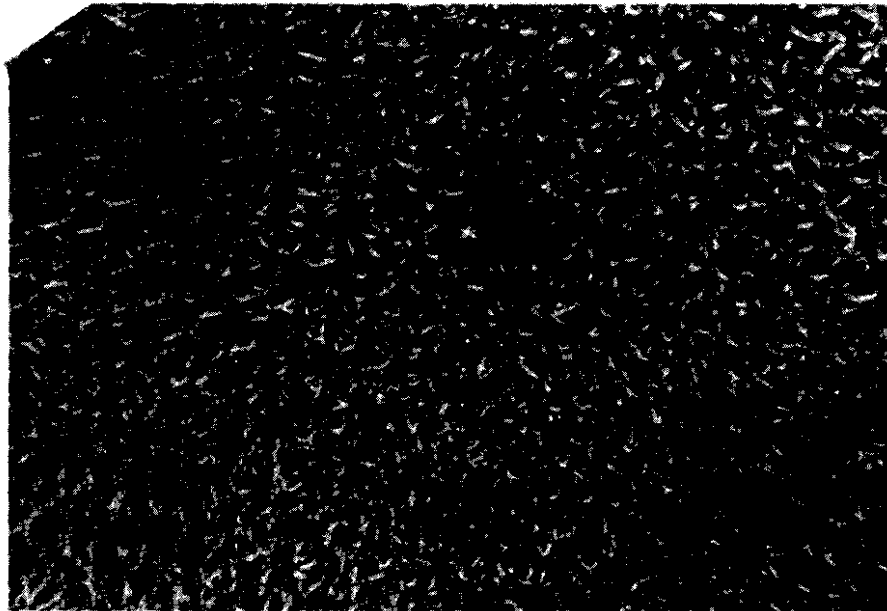
Figure 15.   Overhead View of the PERMA-GRASS.
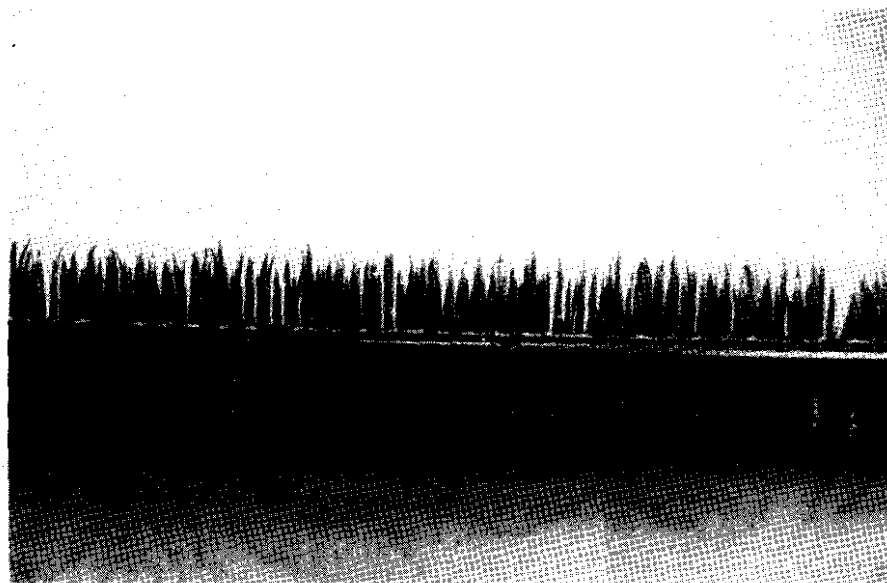
Figure 16.   Side View of a Narrow Strip of
                      PERMA-GRASS.

illustrated in Figure 17 were dry. The water flowed in the
pattern illustrated in Figure 18a. At other times these low
flows were observed in the pattern displayed in Figure 18b,
with a small percentage of the flow passing through the
centers of the tufts of grass.

When the uniform flows were very small in magnitude
with small depths, a type of flow, hereafter called constant-
velocity, was encountered which can be predicted with an
equation similar to that applicable to Darcy flow, the type
of flow which occurs through a porous medium.

The equation for depth prediction for the constant-
velocity flow can be expressed in general form as

$$Y = (K_{cv}) (Q) \tag{12}$$

where K_{cv} is a function of slope. The values of K_{cv} for
the surface material studied are 13.2, 11.0, 7.97, and 6.60
for channel slopes of one, two, three, and four per cent,
respectively. A general equation for depth with respect to
slope and discharge in the constant-velocity regime, for
the experimental surface can be written as:

$$Y = [15.17 - (2.14) (S_o\%)] Q \tag{13}$$

where $S_o\%$ is the bottom slope expressed in per cent. The
individual equations for each slope, rather than the above
general equation, were used to predict the water surface
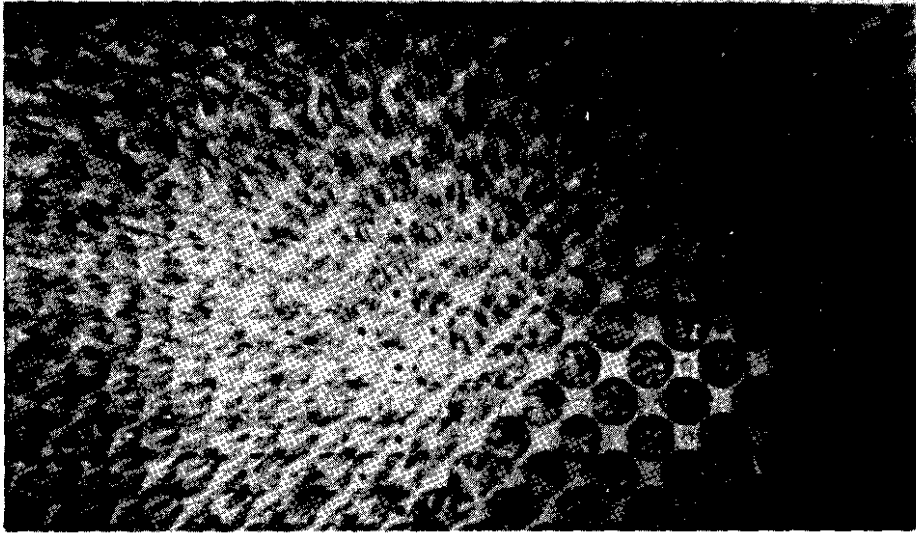
profiles for spatially varied flow.

Mixed Flow

The general depth equation for mixed turbulent and laminar flow can be written as

$$Y = (K_M)(Q)^M \tag{14}$$

where K_M and M vary with the slope. This represents the transitional flow regime between the constant-velocity regime and the turbulent regime. The depth equations for the channel and slopes studied are:

$$1\% \qquad Y = .303 \; Q^{.284}$$
$$2\% \qquad Y = .378 \; Q^{.359}$$
$$3\% \qquad Y = .424 \; Q^{.4005}$$
$$4\% \qquad Y = .453 \; Q^{.428}$$

The upper and lower limits of mixed flow were determined graphically as the range where the data failed to conform to

(a)   (b)
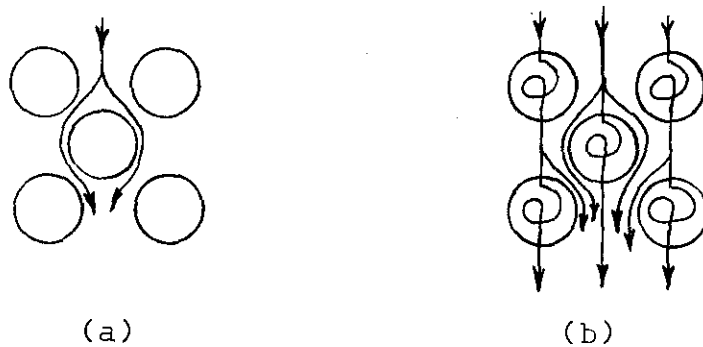
Figure 18.   The Pattern of Flow at Low
             Flows With (a) No Flow
             and (b) Very Little
             Flow, Through the
             Tufts.

the constant-velocity and turbulent flow relationships be-
tween discharge and depth. The constants K_M and M in the
equation $Y = (K_M) (Q)^M$ were then determined from the rela-
tionship of discharge and depth values between the upper
and lower limits of mixed flow.

From linear regressions of K_M and M with S_o%, the
general equations for K_M and M are:

$$K_M = .303 + .249 \log (S_o\%)$$

and

$$M = .284 + .244 \log (S_o\%)$$

The depth equations for specific slopes were used in
making predictions of water surface profiles for spatially
varied flows.

Turbulent Flow

The general depth equation for turbulent flow can be
written as

$$Y_{ef} = (K_T) (Q)^{0.6} \tag{15}$$

where Y_{ef} is the effective depth. An effective bottom was
desired upon which the effective depths of this equation
and the Manning Equation could be based. In order to find
an effective bottom for turbulent flow, water surface
elevation was plotted against $Q^{0.6}$. A value for the
effective bottom was obtained from a linear regression of
the observations on the straight line portion of the plot.
This line extended to $Q^{0.6}$ equal to zero located the effect-
ive bottom elevation. The physical depths for the one, two,

three, and four per cent bottom slopes are greater than the effective depths by approximately .0589, .0569, .0576, and .0613 feet, respectively.

Manning's Equation was used to calculate the values of Manning's n for the uniform flows. A wetted perimeter of $(2Y_{ef} + b)$ was used. Since the effective depth is less than the physical depth and there is much surface contact between the water and the grass blades, the calculated wetted perimeter should be considered the effective, not the real, wetted perimeter.

The uniform flow, average n values computed for the one, two, three, and four per cent bottom slopes are .0325, .0359, .0358, and .0304, respectively. The values indicate that some critical slope is exceeded in going from three to four per cent because of the decrease in the average n values between these two slopes. The values of n tend to decrease as discharge and depth increases. A least squares computer program was used to develop three types of equations for predicting the Manning n for a given Q at a given slope. The best-fit equations, based on the smallest error between predicted compared to observed values, are not all of the same type. These equations for the respective slopes are:

$$1\% \qquad n_p = \frac{Q}{-.02686 + (31.564)\ Q}$$

$$2\% \qquad n_p = \frac{Q}{-.07796 + (29.898)\ Q}$$

$$3\% \qquad n_p = .03774 - (.03767)\ Q$$

$$4\% \qquad n_p = \frac{.02508}{(.06335)\ Q}$$

where n_p is the predicted n value. The maximum errors between the predicted and the observed values for n for the one, two, three, and four per cent channel slopes are respectively one, three, one, and three per cent. However, the predicted values are usually much closer to the observed values than these maximum errors. The experimental and the predicted values of n are presented in Table I.

Regime Dividing Points

The height of the various sizes of grass blades, the geometry of the grass, and the slope are all influential in determining where the flow changes from constant-velocity to mixed or from mixed to turbulent. The base of the grass is about .04 inches thick. The shorter grass stems are between .65 and .75 inches high, while the taller ones are between .93 and 1.00 inches high. Table II illustrates the effect of the vegetation height on the regime dividing points. Note that the transition from constant-velocity to mixed flow occurs at about the height of the shorter stems, while the transition from mixed to turbulent occurs near the height of the taller stems.

Reynolds numbers (RENO) were determined for the regime transition points. As shown in Table III, the Reynolds numbers at these points increased with increasing slope. These results contradict a statement by King and Brater (15)

TABLE I

MANNING n PREDICTION BASED ON DISCHARGE,

UNIFORM FLOWS

Test	Q CFS	n Station 1-4	n Predicted n_p	Effective Depth Ft
1T15	.0180	.0331	.03325	.0316
1T9	.0205	.0333	.03305	.0344
1T11	.0262	.0329	.03275	.0396
1T16	.0310	.0322	.03258	.0434
1T2	.0372	.0323	.03242	.0486
1T12	.0427	.0318	.03233	.0524
1T8	.0470	.0302	.03227	.0539
1T3	.0493	.0319	.03224	.0574
1T4	.0502	.0319	.03223	.0581
1T23	.0550	.0329	.03218	.0626
1T27	.0575	.0329	.03216	.0644
1T28	.0588	.0329	.03215	.0654
1T26	.0633	.0327	.03211	.0681
1T22	.0724	.0324	.03206	.0737
1T24	.0762	.0319	.03204	.0754
1T25	.0798	.0322	.03202	.0779
1T21	.0891	.0315	.03199	.0823
2T9	.0184	.0388	.03897	.0284
2T10	.0221	.0388	.03792	.0317
2T11	.0282	.0368	.03685	.0356
2T12	.0324	.0365	.03637	.0386
2T13	.0382	.0365	.03590	.0427
2T14	.0463	.0352	.03544	.0470
2T15	.0522	.0342	.03521	.0497
2T16	.0592	.0348	.03499	.0544
2T17	.0647	.0350	.03485	.0576
2T18	.0738	.0348	.03467	.0623
2T19	.0780	.0349	.03460	.0646
2T20	.0894	.0344	.03445	.0696
3T9	.0186	.0366	.03704	.0243
3T10	.0221	.0373	.03690	.0273
3T11	.0294	.0362	.03663	.0319
3T12	.0335	.0367	.03648	.0349
3T13	.0381	.0366	.03630	.0377
3T14	.0450	.0362	.03604	.0414
3T15	.0510	.0358	.03582	.0444

TABLE I (Continued)

Test	Q CFS	n Station 1-4	n Predicted n_p	Effective Depth Ft
3T16	.0572	.0358	.03558	.0477
3T17	.0672	.0351	.03521	.0520
3T18	.0723	.0348	.03501	.0542
3T19	.0798	.0343	.03473	.0570
3T20	.0923	.0346	.03426	.0627
4T10	.0227	.0318	.03187	.0231
4T11	.0281	.0314	.03145	.0261
4T12	.0317	.0308	.03121	.0277
4T13	.0389	.0312	.03081	.0317
4T14	.0454	.0311	.03051	.0347
4T15	.0517	.0312	.03025	.0377
4T16	.0564	.0292	.03009	.0382
4T17	.0660	.0292	.02979	.0421
4T18	.0726	.0295	.02961	.0448
4T19	.0773	.0293	.02949	.0465
4T20	.0918	.0296	.02917	.0520

TABLE II

PHYSICAL DEPTH OF FLOW FOR REGIME TRANSITION

POINTS, UNIFORM FLOW

Slope %	Depth, Constant-Velocity to Mixed		Depth, Mixed to Turbulent	
	Ft	In	Ft	In
1	.068	.816	.085	1.020
2	.058	.690	.082	.989
3	.060	.715	.079	.953
4	.061	.729	.082	.988

TABLE III

REYNOLDS NUMBERS AND FLOWS AT REGIME

TRANSITION POINTS, UNIFORM FLOW

Slope %	Constant-Velocity to Mixed		Mixed to Turbulent	
	Q in CFS	Reynolds No	Q in CFS	Reynolds No
1	.0052	375	.0114	821
2	.0062	480	.0143	1164
3	.0074	615	.0152	1212
4	.0091	753	.0187	1560

that there is a tendency for turbulent flow to begin at lower Reynolds numbers at greater slopes.

Equations relating RENO to channel slope were found for the experimental surface to define the transition points from constant-velocity to mixed and from mixed to turbulent. These equations are:

$$\text{Constant-velocity to mixed, RENO} = 248 + 127 (S_o\%) \quad (16)$$

and

$$\text{Mixed to turbulent, RENO} = 576 + 245 (S_o\%) \quad (17)$$

Spatially Varied Flow Water
Surface Profile Prediction

The water surface profiles were predicted for about 25 of the 80 spatially varied flow tests. Predictions were made for the constant-velocity, mixed, and turbulent regimes for various tests. The uniform flow results were used to define the regime transition discharges, though the impact of the falling water probably caused turbulence at slightly lower flows.

Low Flows

The predicted and observed physical depths of various constant-velocity and mixed regime, spatially varied flow tests are displayed in Table IV. As previously stated, at very low flows surface tension effects can cause relatively large errors in depth measurement. For the low flows

TABLE IV

WATER SURFACE PREDICTION FOR LOW, SPATIALLY VARIED FLOW TESTS

Test No	F Type*	Station #11 Exper	Station #11 Pred	F Type	Station #21 Exper	Station #21 Pred	F Type	Station #31 Exper	Station #31 Pred	F Type	Station #40 Exper	Station #40 Pred
1TS1	C	.015	.0139	C	.028	.0265	C	.043	.0403	C	.045	.0504
1TS2	C	.015	.0130	C	.0265	.0248	C	.041	.0366	C	.0425	.0472
1TS11	C	.0505	.0350	C	.0670	.0668	M	.0785	.0754	M	.0800	.0811
1TS12	M	.0785	.0769	M	.082	.0830	T	-----	-----	T	-----	-----
1TS17	M	.0760	.0755	M	.0780	.0790	M	.083	.0821	M	.084	.0847
2TS1	C	.0140	.0156	C	.0274	.0298	C	.0375	.0440	C	.050	.0568
2TS7	M	.0645	.0655	M	.0730	.0728	M	.0763	.0791	T	-----	-----
3TS1	C	.0003	.0038	C	.004	.0074	C	.008	.0109	C	.0115	.0141
3TS16	C	.024	.0226	C	.047	.0432	C	.057	.0613	M	.0665	.0679
3TS17	C	.058	.0605	M	.068	.0675	M	.073	.0739	M	.0775	.0790
4TS1	C	.019	.0185	C	.038	.0353	C	.050	.0522	M	.052	.0636
4TS2	C	.0565	.0584	M	.0650	.0672	M	.069	.0735	M	.076	.0787
4TS8	C	.008	.0096	C	.017	.0185	C	.025	.0273	C	.026	.0352

*F Type refers to flow types, which will be abbreviated: Constant-velocity, C, Mixed, M, and Turbulent, T

64

encountered at the upper end of the channel during low
intensity rainfall, the per cent depth errors may thus be
large because of surface tension effects though the differ-
ences are small in magnitude. Also, there was some varia-
tion in the output of the sprinklers and this non-uniformity
could have caused some error. Considering the magnitude of
the depths that are being predicted and that relations de-
veloped from uniform flow tests are being used to predict
the spatially varied flow results, the predicted values
adequately represent the observed values.

Turbulent Flow Manning n Determination

Several methods were used to determine Manning n values
for use in predicting the water surface profiles for the
spatially varied flow tests. The Manning equation, using
average values between adjacent stations, was used as one
method. Two different values of the Manning n were calcu-
lated using the Manning equation by defining the hydraulic
radius in two ways. In the first method the hydraulic
radius was defined as equal to the depth, while in the
second method it was defined as the area divided by the
wetted perimeter. Manning n values were calculated using
the simplified momentum equation 19 and the energy equation
20.

The Manning n values calculated with the simplified
momentum and energy equations were almost identical. Also,
these values were all within about 0.3 per cent of the
Manning n values calculated with the Manning equation where

the hydraulic radius was defined as equal to the area divided by the wetted perimeter. Therefore, Table V, which lists the Manning n values for the spatially varied flow tests, lists the results of these three methods under one heading, $R = \frac{A}{Wp}$.

A comparison of the Manning n values assuming the hydraulic radius equal to the depth to those calculated using the true hydraulic radius, shows that the values in general, differ by about 5 per cent. This suggests, that for the channel width used in these tests, the assumption that the hydraulic radius is equal to the depth is not a valid assumption and that Manning n values based on this assumption may not adequately predict the water surface profiles.

A comparison of the uniform flow with the spatially varied flow Manning n values in Table V, both based on calculations with the hydraulic radius equal to area divided by wetted perimeter, reveals that the impact of the falling water appears to cause an increase in the n value. Generally this increase is on the order of one to five per cent, though one value was as high as 12 per cent. The intensity of rainfall does not seem to have much effect on the value increase, though there is a trend for the higher intensities to produce a greater increase. The n values consistently decrease as flow or depth increases.

A plotting of the uniform flow (UF) versus spatially varied flow (SVF) n values is presented in Figure 19. Also,

TABLE V

MANNING n VALUES COMPARED FOR SPATIALLY VARIED FLOWS

AND EQUIVALENT UNIFORM FLOWS

Test No	Q Avg CFS	Intensity Inches/Hr	$R = Y_{ef}$	Manning n R = A/WP	**Unif Flow
1TS4	0.02230	2.6	.0351	.0338	.0331
1TS5	0.04176	2.6	.0346	.0329	.0313
1TS8	0.02208	1.3	.0350	.0338	.0333
1TS9	0.03578	1.3	.0343	.0328	.0323
1TS10	0.05522	1.3	.0347	.0326	.0329
1TS13	0.02556	8.0	.0353	.0339	.0329
1TS14	0.04143	8.0	.0345	.0327	.0314
1TS15	0.05451	8.0	.0348	.0328	.0329
1TS18	0.02390	4.0	.0348	.0335	.0330
1TS19	0.03911	4.0	.0349	.0332	.0319
1TS20	0.05637	4.0	.0350	.0329	.0329
2TS3	0.02209	4.0	.0424	.0411	.0388
2TS4	0.03838	4.0	.0409	.0392	.0365
2TS5	0.05319	4.0	.0392	.0372	.0343
2TS8	0.02857	8.0	.0395	.0381	.0368
2TS9	0.04006	8.0	.0375	.0359	.0361
2TS10	0.05176	8.0	.0373	.0355	.0341
2TS13	0.02322	2.3	.0402	.0390	.0384
2TS14	0.03636	2.3	.0384	.0369	.0365
2TS15	0.05951	2.3	.0382	.0361	.0348
2TS18	0.02541	1.3	.0401	.0389	.0377
2TS19	0.03643	1.3	.0382	.0367	.0365
2TS20	0.05456	1.3	.0380	.0361	.0344
3TS8	0.02174	2.6	.0389	.0379	.0365
3TS9	0.03633	2.6	.0383	.0369	.0366
3TS12	0.02262	4.0	.0397	.0386	.0365
3TS13	0.03834	4.0	.0385	.0371	.0366
3TS18	0.04493	8.0	.0378	.0363	.0362
3TS19	0.02593	8.0	.0407	.0394	.0361
3TS20	0.05185	8.0	.0385	.0368	.0358

TABLE V (Continued)

Test No	Q Avg CFS	Intensity Inches/Hr	R = Y_{ef}	Manning n R = A/WP	**Unif Flow
4TS3	0.02773	8.0	.0319	.0311	.0314
4TS4	0.03926	8.0	.0338	.0327	.0312
4TS5	0.06351	8.0	.0342	.0328	.0292
4TS6	0.02318	4.0	.0337	.0329	.0318
4TS7	0.03507	4.0	.0335	.0325	.0311
4TS14	0.02395	2.6	.0336	.0328	.0317
4TS15	0.03803	2.6	.0341	.0330	.0312
4TS19	0.02428	1.3	.0340	.0332	.0317
4TS20	0.03232	1.3	.0336	.0326	.0308

**Uniform flow n values are based on calculations with hydraulic radius equal A/WP and Q = Q Avg of spatially varied flow tests.
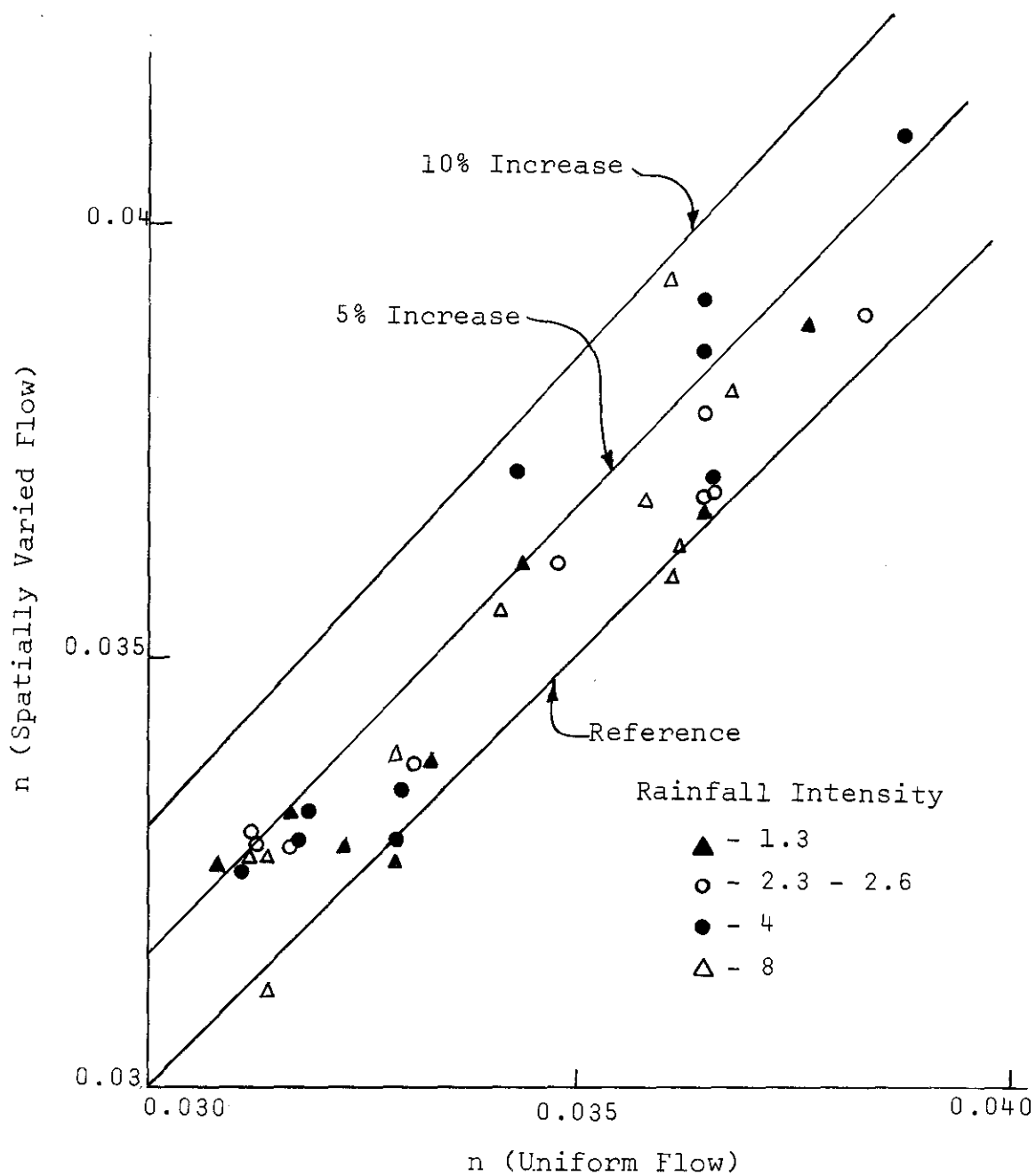
Figure 19.   Relation Between Spatially Varied Flow
n Values and Uniform Flow n Values.

the SVF n values are identified with respect to rainfall intensity. The reference line represents the location where the UF and SVF n values are equal. Lines are also drawn representing variations of 5 and 10 per cent in the UF and SVF n values.

The plotting shows that in general, the SVF n values are greater than the UF n values and that about 80 per cent of the SVF n values differ from the UF n values by less than 5 per cent. Also, the scatter of the points indicates that there is no definable relation between rainfall intensity and the SVF n values.

Turbulent Flow Momentum and Energy Equations

In order to solve the momentum equation, Equation 11, on the computer, it was expanded to the following computational form:

$$
\Delta Y = \left[\frac{(Q_0 - (r)(\Delta x)(\phi))\left(\dfrac{Q_0 - (r)(\Delta x)(\phi)}{(b)(Y_r)} + \dfrac{Q_0 - (r+1)(\Delta x)(\phi)}{(b)(Y_{r+1})} \right)}{(g)(2Q_0 - (2r+1)(\Delta x)(\phi))} \right] \cdot
$$

$$
\cdot \left[\frac{Q_0 - (r+1)(\Delta x)(\phi)}{(Y_{r+1})(b)} - \frac{Q_0 - (r)(\Delta x)(\phi)}{(Y_r)(b)} + \frac{(Q_0 - (r+1)(\Delta x)(\phi))(\phi)}{(Y_{r+1})(b)(Q_0 - (r)(\Delta x)(\phi))} \right] +
$$

$$
+ \left[S_0 \frac{\left[(Q_0 - (r)(\Delta x)(\phi) + (Q_0 - (r+1)(\Delta x)(\phi) \right]^2}{2} n^2}{2.21 \left(\dfrac{b(Y_r + Y_{r+1})}{2} \right)^2 \left(\dfrac{(\frac{b}{2})(Y_r + Y_{r+1})}{(b + Y_r + Y_{r+1})} \right)^{4/3}} \right] \cdot
$$

$$
\cdot \left[\Delta x \right] \tag{18}
$$

where

Y_r = depth at a downstream station (effective or physical)

Y_{r+1} = depth at the adjacent upstream station

r = feet upstream from downstream reference station

Q_o = flow at downstream reference station

Δx = one foot

ϕ = flow added per foot

Station 40, the location of point gage number 4, served as the reference location and starting point for use with equation 18. The computer program estimated Y_{39} at a distance Δx, equal to one foot, up the channel. The estimate of Y_{39} was used to solve for a calculated depth change, which was subtracted from Y_{40} to re-estimate Y_{39}. The new Y_{39} was used to recalculate a depth change (ΔY). When the calculated ΔY values ceased to change within a limit of .00001 foot, the last ΔY value was assumed correct and printed out. The accepted value of Y_{39} was determined by subtracting ΔY from Y. This new depth was then used in calculations for Y_{38}. This iterative procedure was continued until the water surface elevation had been computed to station 11, location of point gage 1.

Equation 19 was used to calculate values of the Manning n at the point gage stations for several rainfall tests at each slope. Then, prediction equations for n as a function of distance up the channel were developed for each test. These equations were utilized with the complete

momentum equation 18 to predict the water surface profiles
for a few spatially varied flow tests. These results are
presented in Table VI along with the observed values.
(Only results for the one and two per cent slope are pre-
sented.) A comparison of the predicted and observed values
shows that the two values differ by only small amounts.

Since the complete momentum equation 18 is somewhat
unwieldy to apply and use, a simplified momentum equation
is desirable if it will give results commensurate to the
complete momentum equation 18. Thus, a simplified momentum
equation was developed as follows: The momentum force F_m,
is equal to $Q \rho V$. Then the average pressure, P_m, over the
cross-sectional area A, due to F_m is $Q \rho V/A$. Expressing the
momentum pressure as some height of water, $P_m = \gamma h_m$, gives

$$\gamma h_m = \frac{Q \rho V}{A}$$

or

$$h_m = \frac{Q \rho V}{A \gamma}$$

But, using the relations $\gamma = \rho g$ and $Q = AV$,

$$h_m = \frac{V^2}{g}$$

This represents the momentum at a cross-section expressed
as an equivalent head. Then the momentum contribution be-
tween two stations, 1 and 2, is

$$\Delta h_m = (\frac{V_1^2}{g} - \frac{V_2^2}{g})$$

Thus, we can write the momentum equation 11 in a simplified
form as

TABLE VI

STEADY STATE SPATIALLY VARIED FLOW PROFILE

PREDICTION USING THE COMPLETE MOMENTUM

EQUATION WITH n = f(x)

Test No	Station No	Effective Depth	Predicted Depth
1TS14	11	.0529	.0519
	21	.0520	.0532
	31	.0563	.0559
	40	.0542	.0542
1TS15	11	.0629	.0619
	21	.0615	.0626
	31	.0653	.0650
	40	.0632	.0632
1TS18	11	.0379	.0373
	21	.0375	.0383
	31	.0403	.0402
	40	.0392	.0392
2TS3	11	.0298	.0302
	21	.0315	.0331
	31	.0326	.0357
	40	.0335	.0335
2TS5	11	.0503	.0502
	21	.0505	.0528
	31	.0526	.0552
	40	.0530	.0530
2TS14	11	.0390	.0399
	21	.0411	.0426
	31	.0414	.0445
	40	.0415	.0415

$$\Delta Y = - (\frac{V_1{}^2}{g} - \frac{V_2{}^2}{g}) + S_o \, \Delta x - S_f \, \Delta x \tag{19}$$

The only assumption necessary for the term $(\frac{V_1{}^2}{g} - \frac{V_2{}^2}{g})$ to equal the momentum term $\frac{Q_1 \, (V_1 + V_2)}{g \, (Q_1 + Q_2)} (\Delta V + \frac{V_2}{Q_1} \, \Delta Q)$ in equation 11 is that $A_1 = A_2 = A_{avg}$. This assumption is closely approximated for the rainfall tests reported for the increment of one foot since the rainfall contribution per foot resulted in only a very small depth change.

It is interesting to compare and note the difference between the simplified momentum equation 19, and the energy (Bernoulli) equation which can be written as:

$$\Delta Y = - (\frac{V_1{}^2}{2g} - \frac{V_2{}^2}{2g}) + S_o \, \Delta x - S_f \, \Delta x \tag{20}$$

The comparison shows that the only difference in the two equations is the integer 2 in the velocity terms. This would indicate that possibly the energy equation would be adequate for predicting the water surface profiles for the tests reported herein.

The simplified momentum equation 19 and the energy equation 20 were used to predict the water surface profiles for several one, two, and three percent bottom slope, spatially varied flow tests. The n versus x relations used with the complete momentum equation 18 were also used with these equations. Manning n values from uniform flow tests, at flows equivalent to the average spatially varied flow for a given test, were also used in equations 19 and 20 to predict water surface profiles.

The water surface profile prediction values found using equations 19 and 20 are presented in Table VII for the tests considered.

A comparison of the predicted values by the simplified momentum and the energy equations shows that the values are almost identical for most of the tests. This suggests that the energy equation is adequate for predicting water surface profiles for spatially varied flows similar to those studied in these tests. This assumes that the roughness of the surface material can be defined and expressed as some appropriate parameter.

For most of the tests reported in Table VII the predicted depths using the constant n values from the uniform flow tests agree as well with the observed depths as the predicted depths calculated using n as a function of the distance up the channel. This is probably because of the small depth change that actually occurs along the channel for the spatially varied flows. Since the depth change along the channel is small, the assumption that the flow is uniform is sufficient as will be shown later.

Figure 20 presents a graphical representation of three of the test results presented in Table VII. This plotting makes it easier to compare the predicted results with the observed results than is possible by studying the tabulated values. (In the test descriptions, the left hand number represents the channel nominal slope, the TS identifies the tests as with rainfall, and the last number or numbers iden-

TABLE VII

STEADY STATE SPATIALLY VARIED FLOW PROFILE

PREDICTION USING THE SIMPLIFIED MOMENTUM

AND ENERGY EQUATIONS

Test No	Station No	Effective Depth (Observed)	Predicted Depth (Momentum)	Predicted Depth (Energy)	n Value
1TS14	11	.0529	.0526	.0512	f(x)
	21	.0520	.0538	.0534	f(x)
	31	.0563	.0561	.0559	f(x)
	40	.0542	.0542	.0542	f(x)
1TS14	11	.0529	.0506	.0493	.0314
	21	.0520	.0518	.0514	.0314
	31	.0563	.0549	.0546	.0314
	40	.0542	.0542	.0542	.0314
1TS15	11	.0629	.0625	.0610	f(x)
	21	.0615	.0632	.0628	f(x)
	31	.0653	.0651	.0649	f(x)
	40	.0632	.0632	.0632	f(x)
1TS15	11	.0629	.0622	.0607	.0329
	21	.0615	.0627	.0623	.0329
	31	.0653	.0654	.0652	.0329
	40	.0632	.0632	.0632	.0329
1TS18	11	.0379	.0377	.0369	f(x)
	21	.0375	.0386	.0385	f(x)
	31	.0403	.0403	.0402	f(x)
	40	.0392	.0392	.0392	f(x)
1TS18	11	.0379	.0371	.0363	.0330
	21	.0375	.0376	.0375	.0330
	31	.0403	.0395	.0394	.0330
	40	.0392	.0392	.0392	.0330
2TS3	11	.0298	.0347	.0346	f(x)
	21	.0315	.0352	.0351	f(x)
	31	.0326	.0363	.0363	f(x)
	40	.0335	.0335	.0335	f(x)
2TS3	11	.0298	.0310	.0308	.0388
	21	.0315	.0320	.0319	.0388
	31	.0326	.0333	.0332	.0388
	40	.0335	.0335	.0335	.0388

TABLE VII (Continued)

Test No	Station No	Effective Depth (Observed)	Predicted Depth (Momentum)	Predicted Depth (Energy)	n Value
2TS5	11	.0503	.0513	.0507	f(x)
	21	.0505	.0537	.0533	f(x)
	31	.0526	.0558	.0556	f(x)
	40	.0530	.0530	.0530	f(x)
2TS5	11	.0503	.0503	.0498	.0343
	21	.0505	.0509	.0506	.0343
	31	.0526	.0518	.0514	.0343
	40	.0530	.0530	.0530	.0343
2TS14	11	.0390	.0408	.0404	f(x)
	21	.0411	.0432	.0430	f(x)
	31	.0414	.0449	.0448	f(x)
	40	.0415	.0415	.0415	f(x)
2TS14	11	.0390	.0412	.0410	.0365
	21	.0411	.0416	.0415	.0365
	31	.0414	.0423	.0422	.0365
	40	.0415	.0415	.0415	.0365
3TS8	11	.0276	.0272	.0277	f(x)
	21	.0273	.0269	.0273	f(x)
	31	.0264	.0270	.0272	f(x)
	40	.0274	.0274	.0274	f(x)
3TS8	11	.0276	.0265	.0265	.0365
	21	.0273	.0268	.0268	.0365
	31	.0264	.0272	.0271	.0365
	40	.0274	.0274	.0274	.0365
3TS12	11	.0286	.0277	.0279	f(x)
	21	.0278	.0278	.0277	f(x)
	31	.0283	.0283	.0281	f(x)
	40	.0289	.0289	.0289	f(x)
3TS12	11	.0286	.0268	.0261	.0364
	21	.0278	.0277	.0273	.0364
	31	.0274	.0287	.0283	.0364
	40	.0289	.0289	.0289	.0364
3TS20	11	.0461	.0453	.0443	f(x)
	21	.0448	.0458	.0444	f(x)
	31	.0444	.0468	.0452	f(x)
	40	.0464	.0464	.0464	f(x)

TABLE VII (Continued)

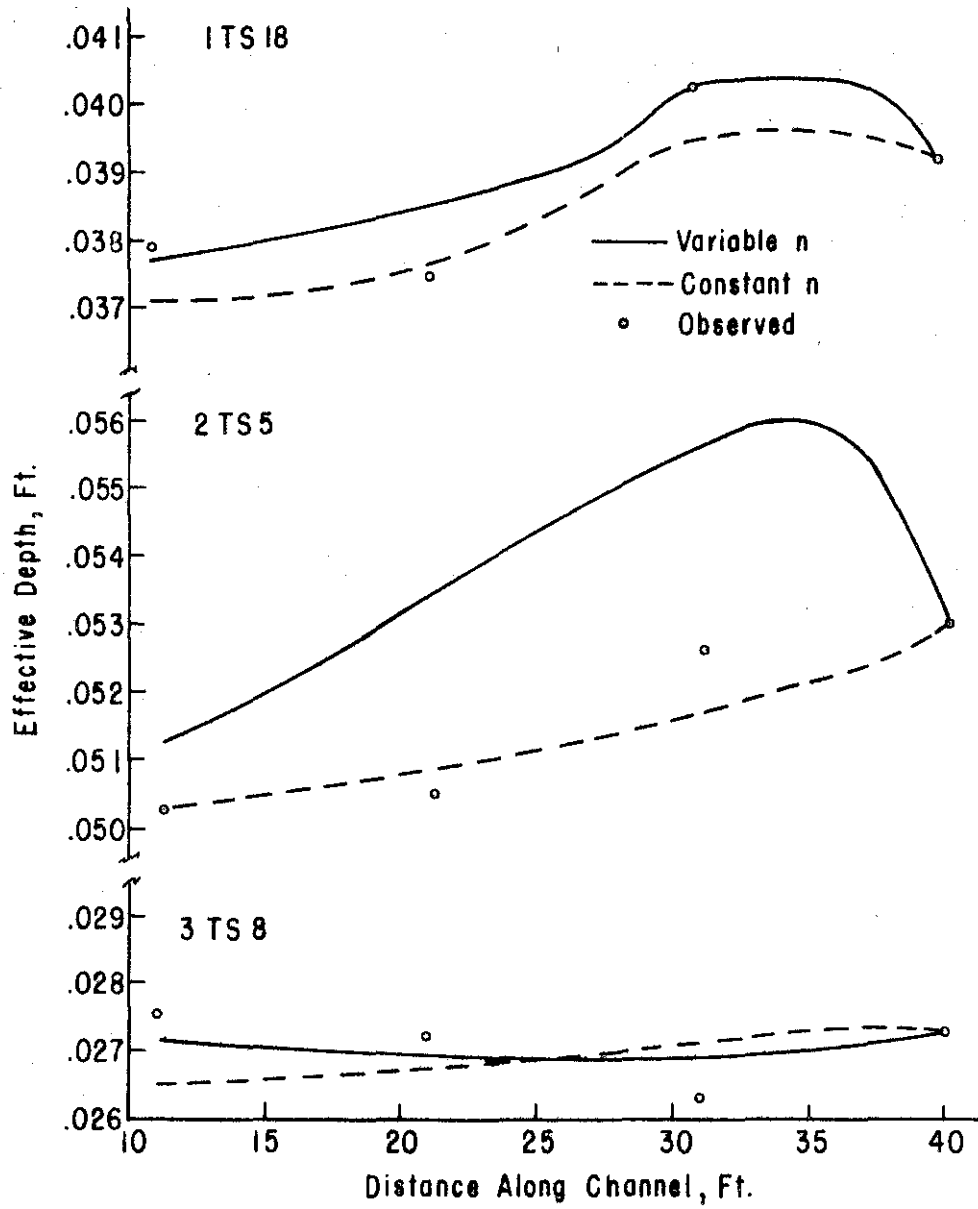| Test No	Station No	Effective Depth (Observed)	Predicted Depth (Momentum)	Predicted Depth (Energy)	n Value
3TS20	11	.0461	.0443	----	.0342
	21	.0448	.0455	----	.0342
	31	.0444	.0468	----	.0342
	40	.0464	.0464	----	.0342

Figure 20. Observed Water Surface Profiles and
Predicted Water Surface Profiles
by Simplified Momentum Equation
19.

tify the test number for the particular slope.)

The plottings show good agreement between the pre-
dicted and observed values for the one and three per cent
slope, but rather poor agreement for the two per cent slope
when n is expressed as a function of distance up the
channel. This appears to be true for all of the tests
considered at the two per cent slope. This is an indi-
cation that the n relation with distance does not adequate-
ly represent the surface roughness at the two per cent
slope.

The uniform flow n value that is equivalent for the
flow with 2TS20 is 0.0358. For this particular test, with
this n value, the friction loss term was so high that a
negative depth was calculated. An n value of 0.0342 gives
a fairly good prediction for the water surface profile for
this test.

Table VIII presents the depth predictions calculated
with the complete and simplified momentum equations using
n as a function of distance up the channel. Either method
does not appear to be significantly superior to the other
with the exception of test 2TS3 for which the complete
equation does predict better than the simplified equation.

The four per cent bottom slope rainfall tests defied
all attempts to predict their profiles. A study of the
data for these tests revealed that the depth at station
four was, on the average, about 20 per cent greater than
the depths at the other three stations. Thus, there is

TABLE VIII

STEADY STATE SPATIALLY VARIED FLOW PROFILE

PREDICTION FOR COMPLETE AND SIMPLIFIED

MOMENTUM EQUATIONS WITH n = f(x)

Test No	Station No	Effective Depth (Observed)	Predicted Depth (Complete)	Predicted Depth (Simplified)
1TS14	11	.0529	.0519	.0526
	21	.0520	.0532	.0538
	31	.0563	.0559	.0561
	40	.0542	.0542	.0542
1TS15	11	.0629	.0619	.0625
	21	.0615	.0626	.0632
	31	.0653	.0650	.0651
	40	.0632	.0632	.0632
1TS18	11	.0379	.0373	.0377
	21	.0375	.0383	.0386
	31	.0403	.0402	.0403
	40	.0392	.0392	.0392
2TS3	11	.0298	.0302	.0347
	21	.0315	.0331	.0352
	31	.0326	.0357	.0363
	40	.0335	.0335	.0335
2TS5	11	.0503	.0502	.0513
	21	.0505	.0528	.0537
	31	.0526	.0552	.0558
	40	.0530	.0530	.0530
2TS14	11	.0390	.0399	.0408
	21	.0411	.0426	.0432
	31	.0414	.0445	.0449
	40	.0415	.0415	.0415

some question as to the accuracy of the data for the four

per cent slope. The results indicate that possibly a gage

zero was in error or that one of the points in the point

gages used to measure the water surface elevation in the

gage wells slipped in the gage. Therefore, the data for the

four per cent slope should be accepted only with skepticism.

Turbulent Flow Simplified Manning Equation

When the energy slope is assumed equal to the bottom

slope and with $Q = AV$, the Manning Equation, Equation 1, can

be written in the following form:

$$A^2 R^{1.33} = \frac{Q^2 n^2}{(1.486)^2 S_o}$$

Since $A = (bY)$ and $R = \frac{(bY)}{(b + 2Y)}$, the Manning Equation may

be written:

$$\frac{b^2 Y^2 b^{1.33} Y^{1.33}}{(b + 2Y)^{1.33}} = \frac{Q^2 n^2}{(1.486)^2 S_o}$$

Solving for the square root of each side of the equation

yields:

$$\frac{(bY)^{1.67}}{(b + 2Y)^{0.67}} = \frac{Q n}{(1.486) (S_o)^{0.5}}$$

Since b is constant, an equation can be developed as:

$$Y = f\left[\frac{(bY)^{1.67}}{(b + 2Y)^{0.67}}\right] = f\left[\frac{Q n}{(1.486) (S_o)^{0.5}}\right]$$

$$= f (G) \tag{21}$$

where G is equal to the terms within the brackets. This equation makes possible the calculation of depth as a function of G. From a computer least squares program, the specific equation for the experimental surface is:

$$Y = .94787 \ (G)^{.61507} \tag{22}$$

For any test the values of Q and S_o are known at the stations along the channel and if the values of n are assumed the same as in equivalent discharge uniform flows, G can be calculated, and the depth then predicted with Equation 22.

A graph relating Y and G was constructed and was utilized in predicting Y for several spatially varied flow tests' results in Table IX. The results presented in Table IX show that the predicted values agree fairly well with the measured values. The predicted values by this method are based on the assumption of uniform flow in the channel. These results suggest that the Manning equation is as acceptable as either the momentum or energy equations for predicting the water surface profiles for vegetated surfaces subjected to low-impact rainfalls and the low flows generally encountered in overland flow.

It is interesting to note that use of the Manning equation in the above described manner for predicting water surface profiles does not require that the depth be known or that one must start at some downstream station. It can be applied to any station along the channel if Q, S_o, b, and some appropriate n value is known.

TABLE IX

GRAPHICALLY PREDICTED VALUES OF DEPTH BY THE SIMPLIFIED
MANNING EQUATION AND MEASURED DEPTHS

Test No	Station No	Effective (Measured)	Depth (Graph)	Physical (Measured)	Depth (Graph)
1TS14	11	.0529	.0498	.1105	.1087
	21	.0520	.0515	.1105	.1104
	31	.0563	.0537	.1160	.1126
	40	.0542	.0554	.1140	.1143
1TS15	11	.0629	.0607	.1205	.1196
	21	.0615	.0620	.1200	.1209
	31	.0653	.0633	.125	.1222
	40	.0632	.0646	.123	.1235
1TS18	11	.0379	.0370	.0955	.0959
	21	.0375	.0379	.0960	.0968
	31	.0403	.0390	.1000	.0979
	40	.0392	.0400	.0990	.0989
2TS3	11	.0298	.0312	.0875	.0881
	21	.0315	.0323	.0884	.0892
	31	.0326	.0333	.0875	.0902
	40	.0335	.0342	.0915	.0911
2TS5	11	.0503	.0503	.1080	.1072
	21	.0505	.0509	.1074	.1078
	31	.0526	.0514	.1075	.1083
	40	.0530	.0520	.1110	.1089
2TS14	11	.0390	.0406	.0967	.09746
	21	.0411	.0415	.098	.09836
	31	.0414	.0420	.0963	.09886
	40	.0415	.0425	.099	.09939
3TS8	11	.0276	.0271	.084	.08470
	21	.0273	.0275	.0855	.08510
	31	.0264	.0279	.085	.08550
	40	.0274	.0280	.0845	.08560
3TS12	11	.0286	.027	.0850	.08460
	21	.0278	.028	.0860	.08560
	31	.0274	.029	.0860	.08660
	40	.0289	.0297	.0860	.08730
3TS20	11	.0461	.044	.1025	.1016
	21	.0448	.0452	.1030	.1028
	31	.0444	.0462	.1030	.1038
	40	.0464	.0472	.1035	.1048

CHAPTER VI

SUMMARY AND CONCLUSIONS

Summary

Uniform and spatially varied flows over a simulated vegetated surface were investigated in a 1.325-foot wide indoor flume at channel slopes of one, two, three, and four per cent. Uniform flow tests were conducted with flows from about 0.1 to 42 gallons per minute, while total flow in the rainfall tests varied from about 0.7 to 27 gallons per minute. Rainfall rates varied from 1.3 to 8 inches per hour. Three flow regimes were observed and were noted as constant-velocity, mixed, and turbulent.

Equations relating depth to flow for each slope were developed for the uniform flows in the constant-velocity and mixed regimes. The relative success of these equations in predicting the water surface profile for increasing steady spatially varied flow is shown in Table IV. Errors in flow or depth measurement could be responsible for the slight differences between measured and predicted values.

Several methods were employed in predicting the water surface profiles for turbulent steady state spatially varied flow. Constant Manning n values from equivalent discharge uniform flow tests, n values from the spatially varied flow

tests and selected constant n values were experimented with in various prediction methods.

The complete and simplified momentum equations and the energy (Bernoulli) equation adequately predicted the water surface profiles. The simplified momentum equation is more easily useable and less cumbersome than the complete momentum equation. Both the momentum equation and the energy equation appear to predict the water surface profiles equally well.

The Manning equation, with the assumption that the energy slope can be represented by the bottom slope, successfully predicted water surface profiles for the steady state increasing spatially varied flows using Manning n values from equivalent uniform flows.

Conclusions

1. For the experimental surface studied the depth can be predicted in the constant-velocity and mixed flow regimes of overland flow from the relationships of Y versus Q obtained from the uniform flow tests.
2. The energy and momentum equation adequately predicted the water surface profiles in the upstream direction. The simplified momentum equation is easy to use and predicted the water surface profiles as accurately as the complete momentum equation.
3. The raindrop impact caused an increase in the roughness for spatially varied flows compared to the uniform

flows. The presence of rainfall, more than the intensity, seemed to affect the roughness, so that no relationship between rainfall intensity and Manning n could be derived.

4. When the bottom slope was assumed equal to the energy slope and equivalent uniform flow Manning n values were used in the Manning Equation, good predictions of the water surface profile for turbulent steady state increasing spatially varied flow resulted for these tests.

Suggestions for Future Study

1. A distribution system giving a simulated rainfall having drop sizes and drop velocity which more closely approximate those of real rainfall would be desirable. The larger drop sizes and greater drop velocities would have a more realistic effect on the roughness and flow depth.

2. A study with base flow of much greater volume over the PERMA-GRASS would indicate the applicability of the momentum and energy equations in predicting the water surface at higher flows than those employed in these tests.

3. The output pressure of the pump for the rainfall distribution system tended to decrease with time and had to be adjusted. A more suitable pump or some other means of maintaining constant pressure would insure minimum variations in drop velocity and rainfall inten-

sity.

4. The PERMA-GRASS was rigid and did not bend over apprec-
   iably even when the flow depth was greater than the
   height of the grass. A study using a more flexible
   grass substitute would illustrate the effect of bending
   of the grass on the surface roughness.

5. The simplified method for predicting the water surface
   worked well for the low-velocity, small-drop rainfalls
   of these tests with a PERMA-GRASS surface. A study of
   higher momentum rainfalls and various simulated vege-
   tated surfaces would reveal how generally the simplified
   method could be applied.

6. A study of the unsteady state spatially varied flow
   profiles of these tests and other tests with different
   simulated vegetated surfaces and different rainfall
   intensity and drop velocity is needed.

7. The drift of the Sanborn was greater than the depth
   measured for some small depths of flow. An accurate
   continuous depth measuring system which is not subject
   to drift would facilitate study of the hydrographs.

8. Capillary action in the small diameter piezometer tubes
   resulted in depth measurement difficulties for very
   small flow depths. Larger diameter tubes would reduce
   this difficulty.

A SELECTED BIBLIOGRAPHY

1. Brakensiek, D. L. "A Report on an Approximate Flood Routing Method." Special Report, United States Hydrograph Laboratory, Beltsville, Maryland.

2. Carter, R. W., et al. "Friction Factors in Open Channels." Proceedings of the American Society of Civil Engineers, Journal of Hydraulics Division. 89:97-143, No. HY2, March, 1963.

3. Chen, Chen-lung and V. E. Hansen. "Theory and Characteristics of Overland Flow." Transactions of the American Society of Agricultural Engineers. 9:20-26, No. 1, 1966.

4. Chow, Ven Te. Open Channel Hydraulics. New York: McGraw-Hill Book Company, Inc., 1959.

5. Daniels, F. and R. A. Alberty. Physical Chemistry. New York: John Wiley and Sons, Inc., 1955.

6. Harbaugh, T. E. "Time Distribution of Runoff From Watersheds." Unpublished Ph.D. dissertation, University of Illinois, 1966.

7. Henderson, F. M. Open Channel Flow. New York: The MacMillan Company, 1966.

8. Horton, R. E., R. Van Vliet, and H. R. Leach. "Laminar Sheet Flow." Transactions of American Geophysical Union. 15:393-404, 1934.

9. Horton, R. E. "The Interpretation and Application of Runoff Experiments with Reference to Soil Erosion Problems." Proceedings, Soil Science Society of America. 3:340-349, 1938.

10. Izzard, Carl F. "Hydraulics of Runoff From Developed Surfaces." Proceedings of the Highway Research Board. 26:129-150, 1946.

11. Izzard, Carl F. "The Surface-Profile of Overland Flow." Transactions of American Geophysical Union. 25:959, 1944.

12. Jumikis, A. R. Introduction to Soil Mechanics. Princeton, New Jersey: D. Van Nostrand Company, Inc., 1967.

13. Keulegan, G. H. "Determination of Critical Depth in Spatially Variable Flow." Proceedings of the Second Midwestern Conference on Fluid Mechanics. Ohio State University. 149:65-79, 1952.

14. Keulegan, G. H. "Spatially Variable Discharge Over a Sloping Plane." Transactions of American Geophysical Union. 25:956-959, 1944.

15. King, H. W. and E. F. Brater. Handbook of Hydraulics. 5th ed. New York: McGraw-Hill Book Company, Inc., 1963.

16. Laws, J. O. and D. A. Parsons. "The Relation of Raindrop-Size to Intensity." Transactions of American Geophysical Union. 24:452-460, 1943.

17. McCool, Don K. "Spatially Varied Steady Flow in a Vegetated Channel." Unpublished Ph.D. dissertation, Oklahoma State University, 1965.

18. Parsons, D. A. "Depth of Overland Flow." USDA-SCS, Soil Conservation Technical Paper No. 82. Washington, D. C. U. S. Department of Agriculture, 1949.

19. Ragan, R. M. "Synthesis of Hydrographs and Water Surface Profiles for Unsteady Open Channel Flow with Lateral Inflows." Unpublished Ph.D. dissertation, Cornell University, 1965.

20. Ree, W. O. "An Approach to Hydrology Through Hydraulics." Presented to the Precipitation Congress, St. Louis, Missouri, April 1, 1964.

21. Ree, W. O. "A Progress Report on Overland Flow Studies." Presented to the Soil Conservation Service Hydraulic Engineers Meeting, New York, New York, August 13, 1963.

22. Ree, W. O. "Overland Flow and Direct Runoff." Presented to the Unit Source Watershed Conference, St. Louis, Missouri, February 16, 1965.

23. Robertson, A. F., et al. "Runoff from Impervious Surfaces Under Conditions of Simulated Rainfall." Presented to the Annual Meeting of the American Society of Agricultural Engineers, Fort Collins, Colorado, June 23, 1964.

24. Sweeten, J. M. "The Hydraulic Roughness of an Irrigation Channel with Decreasing Spatially Varied Flow." Unpublished M. S. thesis, Oklahoma State University, 1967.

25. Turner, A. K. "The Simulation of Rainfalls for Studies in Overland Flow." Journal of the Institution of Engineers, Australia. 37:9-15, 1965.

26. Woo, D. C. and E. F. Brater. "Laminar Flow in Rough Rectangular Channels." Journal of Geophysical Research. 66:4207-4218, 1961.

27. Woo, D. C. and E. F. Brater. "Spatially Variable Flow From Controlled Rainfall." Proceedings of the American Society of Civil Engineers, Journal of the Hydraulics Division. 88"31-56, No. HY6, Part 1, November, 1962.

28. Wright, J. L. and E. R. Lemon. "Photosynthesis Under Field Conditions VIII. Analysis of Windspeed Fluctuation Data to Evaluate Turbulent Exchange Within a Corn Crop." Agronomy Journal. 58: 255-261, 1966.

VITA

Paul Keith Rodman

Candidate for the Degree of

Master of Science

Thesis: STEADY STATE INCREASING SPATIALLY VARIED FLOW OVER
A SIMULATED VEGETATED SURFACE

Major Field: Agricultural Engineering

Biographical:

Personal Data: Born in Marshall, Arkansas, February
12, 1945, the son of Toy K. and Kathaleen M.
Rodman.

Education: Graduated from Mary Carroll High School,
Corpus Christi, Texas, in 1963.   Received the
Bachelor of Science degree in Agricultural
Engineering in January, 1968, from Oklahoma State
University.   Completed the requirements for the
Master of Science degree in August, 1969.

Professional Experience: In charge of the water budget
for the Lake Hefner Evaporation Suppression In-
vestigation for one and one-half years as an
undergraduate.   Graduate Research Assistant for
one year for the Agricultural Engineering Depart-
ment, Oklahoma State University.